
How Much Do Circuits Tell Us? Measuring the Consistency and Specificity of Language Model Circuits


Michael Li  Nishant Subramani 

Abstract

The circuits framework in mechanistic interpretability aims to identify causally important sparse subgraphs of model components, typically evaluated by measuring *necessity* and *sufficiency*. We measure circuit reuse, the proportion of components shared across per-example circuits within a task, and investigate two less-studied properties of this: *consistency*, the recurrence of components within a task, and *specificity*, their uniqueness to a task. Using edge attribution patching across six tasks and seven models, we find that within-task reuse is high and that shared components are necessary for task performance, with ablations causing up to $\sim 100\%$ relative accuracy drops. However, circuits turn out not to be task-specific: ablating one task’s circuit damages another task’s performance about as much as that task’s own circuit does. We discover that this is due to substantial overlap between circuits across tasks, which are causally important for performance. Some circuits do contain a smaller set of task-specific components, but these account for only a modest portion of circuit performance. Overall, our findings suggest that while circuit discovery at the level of attention heads and MLP layers identifies important components, their lack of task-specificity raises questions about the degree to which circuits can support targeted understanding and intervention on model behavior.

1. Introduction

Neural networks are infamously black box; even when we can elicit strong performance on a task, it is unclear which internal computations are responsible. The field of mechanistic interpretability seeks to reverse-engineer the internal

 Language Technologies Institute, Carnegie Mellon University, Pittsburgh, Pennsylvania, USA. Correspondence to: Michael Li <ml6@cs.cmu.edu>, Nishant Subramani <nishant2@cs.cmu.edu>.

Preprint. May 12, 2026.

computations of neural networks by identifying *circuits*: sparse subgraphs of model components that are causally responsible for a particular behavior (Elhage et al., 2021; Wang et al., 2023). A growing body of work has developed methods for extracting such circuits (Syed et al., 2024; Marks et al., 2025; Jafari et al., 2025) and evaluating their *necessity* (removing the circuit should degrade performance) and *sufficiency* (the circuit alone should reproduce the behavior) (Shi et al., 2024).

We argue that there are two additional properties that are crucial to consider (Figure 1). First, circuits should be *consistent*: if a circuit truly captures how a model solves a task, the same components should recur for different instances of that task. Second, circuits should be *specific*: a task’s circuit should be meaningfully different from the circuits of unrelated tasks. Without consistency, a circuit is an artifact of a particular input rather than a description of the model’s algorithm. Without specificity, a circuit is not task-specific, limiting its utility for understanding or intervention.

We test both properties at scale. Using Edge Attribution Patching (EAP; Syed et al. (2024)), we extract per-example circuits for $n=1000$ examples across six tasks spanning algorithmic reasoning (Addition, Boolean Logic), information retrieval (IOI, CopyColors MCQA), and knowledge-intensive benchmarks (ARC Easy, ARC Challenge), and seven models from four architecture families (Gemma 2, Llama 3.2, Qwen3, OLMo-2). We find the following:

1. **Circuits are consistent within a task.** Across tasks and models, a substantial fraction of each per-example circuit is drawn from a shared set of components. Ablating this shared set causes large accuracy loss compared to a capacity-matched random ablation, confirming that the shared components are causally important, not merely high-scoring attribution method artifacts.
2. **Circuits are not specific across tasks.** When we ablate one task’s circuit and evaluate on a different task, the performance drop is comparable to ablating that task’s own circuit. This is explained by the substantial overlap between task circuits: at the component level, different tasks’ circuits are composed of largely the same MLP layers. Selective ablation experiments

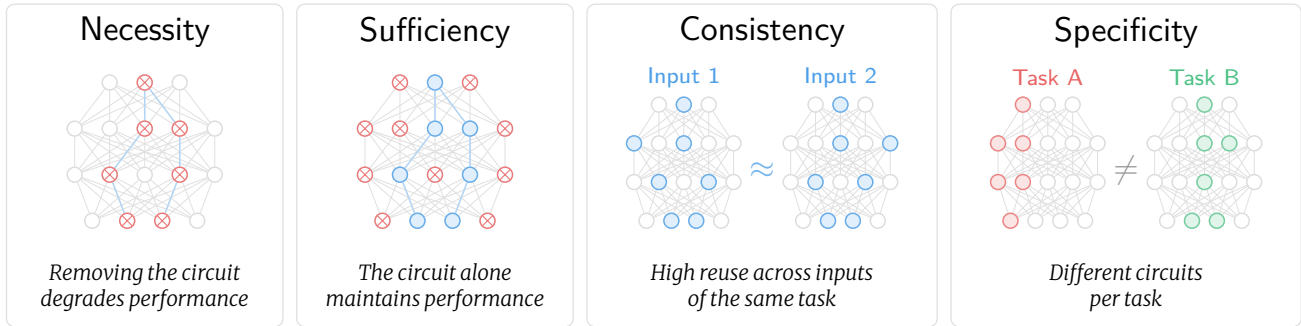


Figure 1. **Circuit evaluation criteria.** We propose evaluating circuits for consistency across inputs and specificity across tasks, in addition to necessity and sufficiency.

reveal that a small number of important task-specific components do exist, but the bulk of each circuit is shared across tasks.

These findings suggest that circuit discovery at the level of attention heads and MLP layers primarily identifies general-purpose model infrastructure rather than task-specific mechanisms. We discuss several explanations for this - including the role of shared MLP layers and polysemanticity - and speculate that finer-grained methods, such as concept-level/sparse feature circuits (Marks et al., 2025), may be needed to recover task-specific structure. We also discuss implications for applications that assume circuit-level modularity, including model editing (Meng et al., 2022; Dai et al., 2022) and safety interventions (Li et al., 2023), while noting important limitations of our analysis for these settings.

2. Background

2.1. Transformer Circuits

We use the Transformer Circuits framework (Elhage et al., 2021) to represent decoder-only transformers as a directed acyclic computational graph. The *residual stream* acts as a central communication channel: the token embedding is written into it, and each subsequent layer reads from it, performs a computation, and additively writes its output back. Because contributions are additive, the output of any component can influence any downstream component, resulting in a fully connected graph between layers. Within this graph, nodes are the model’s computational units, typically attention heads and MLP layers, though other decompositions (e.g., individual neurons or sparse autoencoder features) are also possible (Marks et al., 2025; Arora et al., 2025; Ameisen et al., 2025). Edges represent the flow of information between components through the residual stream. A *circuit* is then defined as a sparse subgraph of this computational graph which is sufficient to explain a given model behavior (Wang et al., 2023; Conmy et al., 2023).

2.2. Edge Attribution Patching

To identify components which are important for a given behavior, researchers typically use activation patching (Vig et al., 2020; Meng et al., 2022; Wang et al., 2023), which replaces each component’s activation with its value under a corrupted input and measures how much the output changes. However, this requires a separate forward pass per component, which becomes prohibitively expensive. Edge Attribution Patching (EAP; Syed et al. (2024)) approximates these causal effects using gradient information, requiring only two forward passes and one backward pass per example. Components are ranked by the absolute value of their attribution score and the top- K components define the circuit. Syed et al. (2024) show that EAP recovers circuits competitive with those found by more expensive methods, making it suitable for the large-scale analysis we conduct here (see §B for the full details).

3. Methodology

3.1. Tasks and Models

We evaluate on six tasks spanning algorithmic reasoning (Addition, Boolean Logic), information retrieval from context (IOI (Wang et al., 2023), CopyColors MCQA (Mueller et al., 2025)), and knowledge-intensive benchmarks (ARC Easy, ARC Challenge (Clark et al., 2018)). Full task descriptions are in §C. We study seven models from four architecture families: Gemma 2 (2B, 2B IT; Gemma Team (2024)), Llama 3.2 (3B, 3B Instruct; Llama team (2024)), Qwen3 (4B, 8B; Yang et al. (2025)), and OLMo-2-1B (Team OLMo, 2024), which is used for pretraining dynamics analysis.

3.2. Extracting and Evaluating Shared Circuits

For each task T we use a dataset $\mathcal{D}_T^{\text{train}} = \{(x_i, y_i)\}_{i=1}^n$ of $n = 1000$ examples, where x_i is an input prompt and y_i the target answer token, and a disjoint held-out evaluation

set $\mathcal{D}_T^{\text{eval}}$. Let $\mathcal{C} = (\mathcal{V}, \mathcal{E})$ denote the model’s computation graph, where vertices \mathcal{V} are model components (attention heads and MLPs) and edges \mathcal{E} are the connections between them. For each $(x_i, y_i) \in \mathcal{D}_T^{\text{train}}$ we extract a per-input circuit $\mathcal{C}_i \subseteq \mathcal{C}$ via EAP, defined as the subgraph spanned by the top- $K\%$ of components by absolute attribution score, and sweep $K \in \{1, 5, 10, 20, 30\}$. Given the per-input circuits $\{\mathcal{C}_i\}_{i=1}^n$, the shared component set (S_P) contains all components that appear in at least P of per-input circuits:

$$S_P = \left\{ c \in \mathcal{C} : \frac{1}{n} \sum_{i=1}^n \mathbf{1}\{c \in \mathcal{C}_i\} \geq P \right\}. \quad (1)$$

We define **reuse@ P** as the mean fraction of a per-input circuit overlapping with the shared set,

$$\text{reuse@}P = \frac{1}{n} \sum_{i=1}^n \frac{|S_P \cap \mathcal{C}_i|}{|\mathcal{C}_i|}, \quad (2)$$

and report **reuse@ P** for $P \in \{95\%, 96\%, \dots, 100\%\}$.

To test whether shared components are causally important, we ablate (zero out) the shared set S_P and measure accuracy on $\mathcal{D}_T^{\text{eval}}$. A raw accuracy drop, however, is difficult to interpret. Removing any set of components reduces network capacity, so some degradation is expected regardless of whether the ablated components are task-relevant. We therefore compare the shared-set ablation against a **capacity-conserved control** (C^3). Let S_C be a uniformly random subset of $\mathcal{C} \setminus S_P$ matching S_P in the number of attention heads and MLPs.¹ Since both ablations are capacity-matched, any additional degradation from the shared-set ablation can largely be attributed to the functional role of those components rather than to capacity.

We formalize ablation via the do-calculus (Pearl, 1995). For an ablation set $S \subseteq \mathcal{C}$, let $\text{do}(S \leftarrow 0)$ denote the intervention that clamps every $c \in S$ to zero. Vertex activations are set to zero, and edges are removed from the computation graph (equivalently, the signal passed along them is zeroed). The model’s output distribution on x under this intervention is $p_{\mathcal{M}}(\cdot | x; \text{do}(S \leftarrow 0))$, with $S = \emptyset$ referring to the output distribution of the original (unablated) model. We define the **zero-ablated prediction** (ZAP) of \mathcal{M} under ablation S as the model’s top-logit token under the intervention,²

$$\text{ZAP}(\mathcal{M}, S, x) = \arg \max_{y'} p_{\mathcal{M}}(y' | x; \text{do}(S \leftarrow 0)), \quad (3)$$

We define accuracy on task T under ablation S as the fraction of held-out examples on which the model’s prediction

¹We do not randomly sample edges; ablating a vertex zeroes out all edges adjacent to it, so matching vertex counts automatically accounts for edge ablation.

²We use argmax decoding here, but any decoding algorithm could be used on the output distribution $p_{\mathcal{M}}$.

equals the true label,³

$$\text{acc}(\mathcal{M}, S) = \frac{1}{|\mathcal{D}_T^{\text{eval}}|} \sum_{(x,y) \in \mathcal{D}_T^{\text{eval}}} \mathbf{1}\{y = \text{ZAP}(\mathcal{M}, S, x)\}. \quad (4)$$

Finally, we define the causal effect of S_P on task T as

$$\text{necessity}(\mathcal{M}, S_P) = \frac{\text{acc}(\mathcal{M}, S_C) - \text{acc}(\mathcal{M}, S_P)}{\text{acc}(\mathcal{M}, \emptyset)}. \quad (5)$$

A positive *necessity* means ablating S_P hurts more than C^3 , which we interpret as evidence that the shared components are causally important for task T .

3.3. Cross-Task Experiments

The experiments above tell us whether the shared components are causally important for a given task. However, they do not disambiguate whether those components are specific to that task. A component could be critical for task A simply because it is critical for all tasks, in which case finding it in task A ’s circuit might not tell us much about task A in particular. To probe specificity, we run two cross-task experiments. The first ablates a task’s shared circuit and measures the effect on other tasks. The second ablates subsets of different task’s circuits.

First, define $\Delta_A^B = \text{acc}_A(\mathcal{M}, \emptyset) - \text{acc}_A(\mathcal{M}, S_P^B)$, the accuracy drop on task A when ablating task B ’s shared circuit, where acc_A denotes accuracy evaluated on $\mathcal{D}_A^{\text{eval}}$ and S_P^B is task B ’s shared component set. If circuits are task-specific, ablating task A ’s own circuit should hurt task A more than ablating any other task’s circuit. For each task and model, we compare Δ_A^A , the drop on A when ablating its own circuit, against $\frac{1}{|\mathcal{T}|-1} \sum_{B \neq A} \Delta_A^B$, the mean drop on A when ablating each other task’s circuit instead.

Second, to localize where task-specific signal resides, we partition the union $\mathcal{C}_A \cup \mathcal{C}_B$ for a pair of tasks (A, B) into three disjoint sets: the *shared core* $\mathcal{C}_A \cap \mathcal{C}_B$ (components in both circuits), the *A-only* set $\mathcal{C}_A \setminus \mathcal{C}_B$ (components in \mathcal{C}_A but not \mathcal{C}_B), and the *B-only* set $\mathcal{C}_B \setminus \mathcal{C}_A$ (components in \mathcal{C}_B but not \mathcal{C}_A). We ablate each set independently and report the accuracy drop on task A alongside the mean drop across other tasks. Results are averaged over all task pairs.

4. Within-Task Consistency

Circuits reuse the same components across inputs. If a circuit captures how a model solves a task, the same components should appear regardless of which input is used. We find consistent evidence for this. Figure 2 (top row) shows the **reuse@97%** rate - the fraction of each example’s

³ S_P , acc , and *necessity* all implicitly depend on T (through $\mathcal{D}_T^{\text{train}}$ and $\mathcal{D}_T^{\text{eval}}$), but we drop T from the notation for readability.

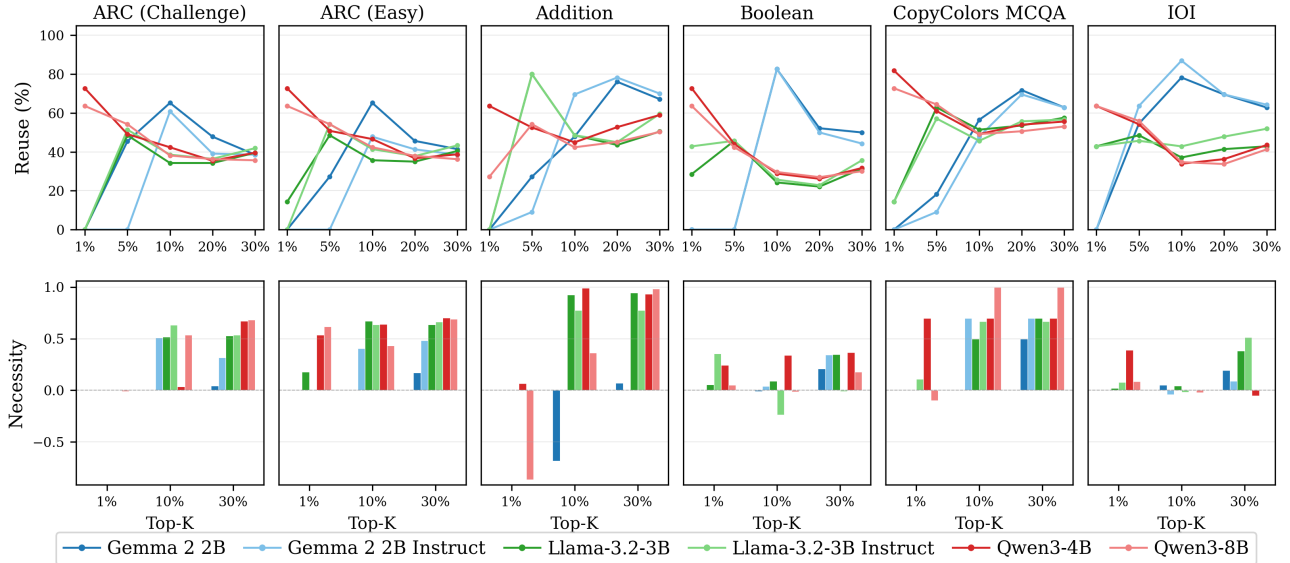


Figure 2. **Within-task circuit reuse and importance scores across circuit sizes.** *Top:* reuse@97% measures the fraction of each example’s top- K % circuit covered by components appearing in at least 97% of examples; each line is a model, and the x -axis sweeps the circuit size K . *Bottom:* The importance score measures how much more performance drops when shared components are removed versus when an equally sized random set is removed; a positive score means the shared components matter more than a random set of the same size. See §E for all settings.

circuit covered by components appearing in at least 97% of examples - as a function of circuit size K , with each model as a separate line (see §E for additional settings). Most task-model combinations show 40-70% reuse at $K=10\%$, meaning that roughly half or more of any individual example’s circuit is drawn from a set of components shared by nearly every example. CopyColors MCQA and Boolean tend toward the higher end, while ARC and IOI are more moderate. The Qwen models generally achieve higher reuse than Llama or Gemma.

The relationship between reuse and circuit size is not strictly monotonic: for some task-model pairs reuse increases with K (e.g., Addition in the Gemma 2 family), while for others (e.g., IOI in the Qwen 3 family) it decreases as the larger circuit pulls in more example-specific components. Despite this variation, reuse remains well above zero at $K \geq 5\%$.

Shared components are actually doing work, not just appearing frequently. High reuse alone does not establish that the shared components matter for the task - they could simply be components with large activations that get ranked highly without playing a real functional role. We test this directly by comparing how much performance drops when the shared components are removed versus when an equally sized set of randomly chosen components is removed. Figure 2 (bottom row) shows this excess performance drop across tasks and models. For most tasks, removing the shared components hurts more than removing an equally sized random set, and this gap grows with K . The effect

is strongest at moderate-to-large circuit sizes ($K \geq 10\%$), where Addition shows an excess drop of 0.8-1.0 across all models and CopyColors MCQA reaches 0.5-0.8.

The one exception is Addition at $K=1\%$ in Gemma models, where the circuit contains only 3 MLPs, making random comparisons somewhat likely to overlap with it by chance.⁴ This disappears at larger K , where Addition shows the largest excess drop of any task.

Consistency emerges early but degrades over training; necessity is largely uninformative until anneal. Figure 3 tracks reuse and necessity across OLMo-2-1B’s full $\sim 4T$ -token training run. reuse@ $P=95$ at $K=10\%$ peaks in the first $\sim 76B$ tokens (around 50–60% for all tasks) and then declines for the rest of stage-1: to 7–22% on Addition, 25–35% on ARC, 18–37% on IOI, and 30–50% on CopyColors MCQA. Most of this drop happens in the gap between our 76B and 399B checkpoints rather than gradually over training. Boolean is the most extreme: its $K=10\%$ shared circuit becomes empty by 399B and remains so for the rest of training. The two anneal checkpoints sit close to the late stage-1 reuse values, suggesting the anneal phase does not substantially reshape circuit consistency.

Necessity is hard to read for most of stage-1 because baseline accuracy on Addition, ARC, and MCQA hovers near chance, leaving little room for ablation to do measurable damage. During the anneal phase however, baselines on

⁴There are 26 MLPs in Gemma 2 2B.

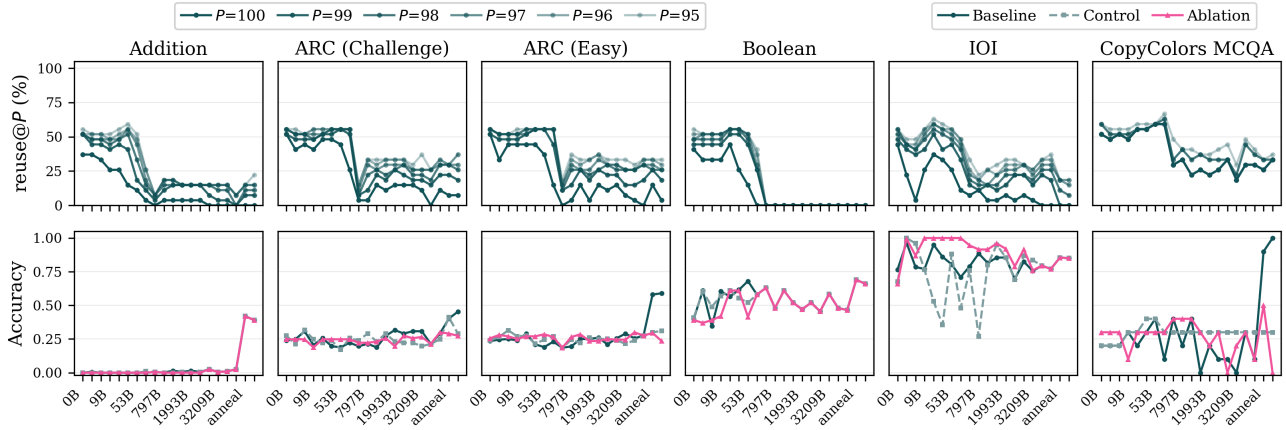


Figure 3. Pretraining dynamics of circuit reuse and causal importance in OLMo-2-1B. Top: reuse@P at $K=10\%$ across pretraining checkpoints, sweeping the consistency threshold $P \in \{95, \dots, 100\}$ (darker = stricter). Bottom: Baseline accuracy (teal solid), accuracy after a capacity-matched random ablation (gray dashed), and accuracy after ablating the shared $K=10\%$ circuit (pink). The gap between gray and pink reflects necessity. Checkpoints span the full training run from 0B to 4001B tokens of stage-1 plus two stage-2 *aneal* checkpoints (`ingredient1`, `ingredient3`); each *aneal* continues training for ~ 51 B more tokens on a curated mixture with a learning-rate decay schedule, producing the released OLMo-2-1B.

MODEL	MLP / ATTN (%)				
	$K=1$	$K=5$	$K=10$	$K=20$	$K=30$
GEMMA-2-2B	100/0	100/0	94/6	53/47	36/64
GEMMA-2-2B-IT	100/0	100/0	97/3	54/46	36/64
LLAMA-3.2-3B	99/1	59/41	33/67	18/82	13/87
LLAMA-3.2-3B-IT	99/1	60/40	34/66	19/81	13/87
QWEN3-4B	100/0	48/52	27/73	14/86	10/90
QWEN3-8B	100/0	53/47	29/71	15/85	10/90

Table 1. Mean of MLP vs. attention head circuit share across tasks.

Addition (0→40%), ARC (Easy) (25→58%), and CopyColors MCQA (10→95%) jump sharply. This is likely because *aneal* mixtures emphasize downstream-task data, and so the model has started learning these tasks. On MCQA at the *aneals*, ablating the shared circuit drops accuracy from $\sim 95\%$ to 0% while a capacity-matched random ablation only drops it to 30%. On ARC, by contrast, both ablations land near 25%, so the circuit is not necessary. Full checkpoint breakdowns are in §L.

MLP layers dominate at small circuit sizes. Breaking down circuits by component type reveals that MLPs make up the vast majority of small circuits (§4; see §G for full results across all models). For Gemma 2 2B-IT, MLPs account for 95-100% of the circuit at $K \leq 10\%$ across all tasks, and the Llama and Qwen families show the same pattern. As K increases, attention heads take up a progressively larger share, reaching roughly half the circuit by $K=20$ -30%. The location of these components across layers varies by model family: in Llama and Qwen, the small- K circuits are concentrated in early layers, with middle- and late-layer

components joining as K grows. Gemma is more task-dependent, with some tasks placing their small circuits in middle-to-late layers instead (see §H for cumulative layer distributions). This is consistent with early work analyzing BERT, which found that lower layers tend to capture general syntactic structure while higher layers specialize in more task-specific semantic processing (Tenney et al., 2019).

5. Cross-Task Specificity

Having established that circuits are consistent, we now ask a different but related question: are the components identified for one task *specific* to that task? We investigate this below.

Removing one task’s circuit damages other tasks just as much, in most models. If circuits are task-specific, removing task A ’s circuit should damage task A far more than task B . For most model families, this is not what we observe. Figure 4 compares, for each task and model at $K=10\%$, the accuracy drop from removing that task’s own circuit (“Own”) against the mean drop from removing all other tasks’ circuits (“Other”; see §F for all K values). These two numbers are close in the Llama and Qwen families: in Llama-3.2-3B, removing the Addition circuit causes a 99% drop on Addition, while removing other tasks’ circuits causes a mean 99% drop on Addition as well. For ARC (Challenge), the own-circuit drop is 41% and the other-circuit mean is 40%. The Gemma family is a notable exception, showing more differentiation between tasks in several cases. For example, CopyColors MCQA in Gemma 2 2B IT has a 68% own-circuit drop vs. 42% from other circuits - a gap large enough to suggest some degree of task-specific structure at this granularity.

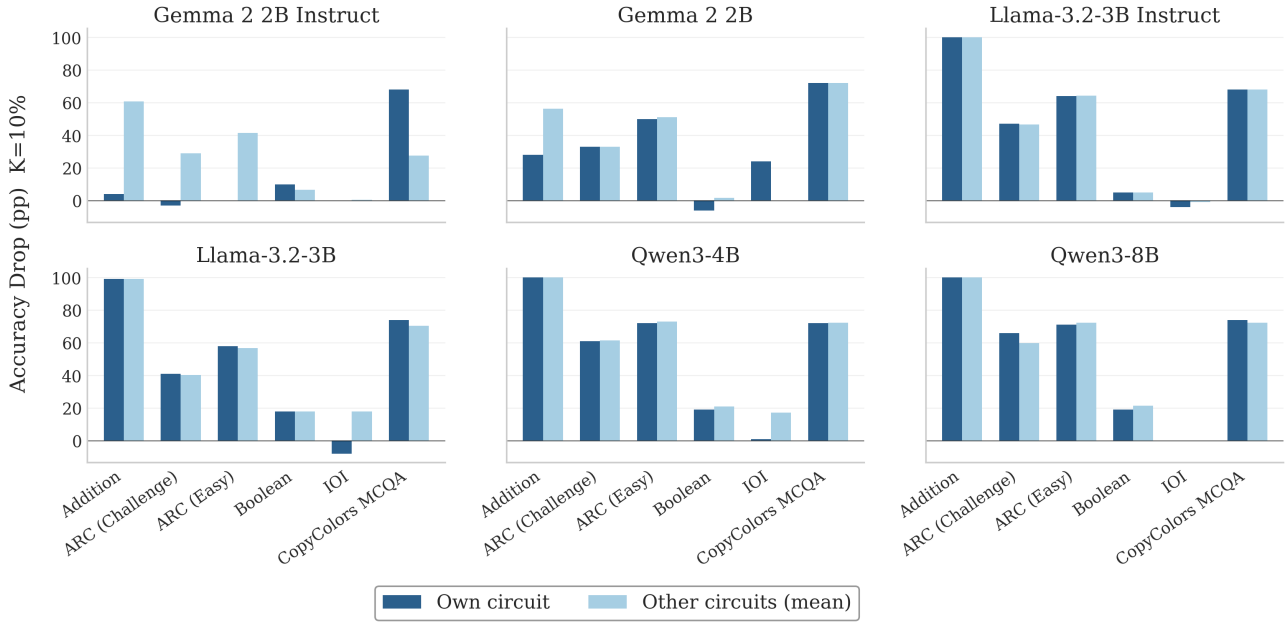


Figure 4. **Own-circuit vs. other-circuit accuracy drop at $K=10\%$.** For each task, “Own” is the accuracy drop from removing that task’s circuit; “Other” is the mean drop from removing every other task’s circuit. The two bars are close across tasks and models, indicating that circuits are not task-specific. See §F for all K values.

The fact that removing *other* tasks’ circuits causes equally large drops on Addition tells us that Addition’s small circuit is not unique to it - it is a subset of the shared components that every task depends on.

The non-specificity is explained by how much circuits overlap. The near-identical accuracy drops are explained by the fact that different tasks’ circuits are composed of largely the same components. Figure 5a shows the overlap between task pairs’ circuits at $K=10\%$ for Llama-3.2-3B and Qwen3-4B (see §F for all K values and models). Overlap at $K=10\%$ typically ranges from 0.46 to 0.89, with the highest overlap between related tasks (ARC Easy and ARC Challenge: 1.00 in Llama, 0.89 in Qwen) and the lowest involving CopyColors MCQA. For comparison, two random circuits of size K would have expected overlap of roughly $K/(2 - K)$, or about 5% at $K=10\%$ - an order of magnitude below what we observe. Overlap tends to be highest at small K and decreases as K grows and more task-specific components enter the circuit, but remains well above chance even at $K=30\%$.

Task-specific structure exists and has measurable effects. High overlap does not mean circuits are entirely undifferentiated. To identify where task-specific structure resides, we split each pair of task circuits into three non-overlapping groups: the shared core (components in both circuits), the task-specific components (in circuit A but not B), and the complementary components (in circuit B but not A). We

then remove each group independently (Figure 5b; see §I for results across all K values and models).

Shared core. Removing the shared core causes large drops on both the target task and other tasks. For Addition in Llama-3.2-3B, removing the shared core drops the target by $\sim 97\%$ and other tasks by $\sim 38\%$; in Qwen3-4B, the pattern is similar ($\sim 83\%$ vs. $\sim 20\%$). For ARC (Challenge), the target and non-target drops are closer ($\sim 37\%$ vs. $\sim 35\%$ in Llama). In all cases, removing the shared core causes substantially more damage than removing an equally sized random set, confirming that these components are genuinely important rather than simply numerous.

Task-specific components. Removing the task-specific components produces larger accuracy drops on the target task than on other tasks, showing that these components carry some signal that is genuinely specific to that task. For Addition, the target drop is larger than the drop on other tasks ($\sim 83\text{pp}$ vs. $\sim 18\text{pp}$ in Llama-3.2-3B), suggesting these components do carry some Addition-specific signal. For ARC and CopyColors MCQA, the gap between target and non-target drops is much smaller. In absolute terms, these components are also small, accounting for only 15–30% of the total circuit at $K=10\%$ (see §J).

Complementary components. Removing the complementary components generally causes small drops that do not disproportionately hurt the target task.

In summary, the shared core accounts for most of each cir-

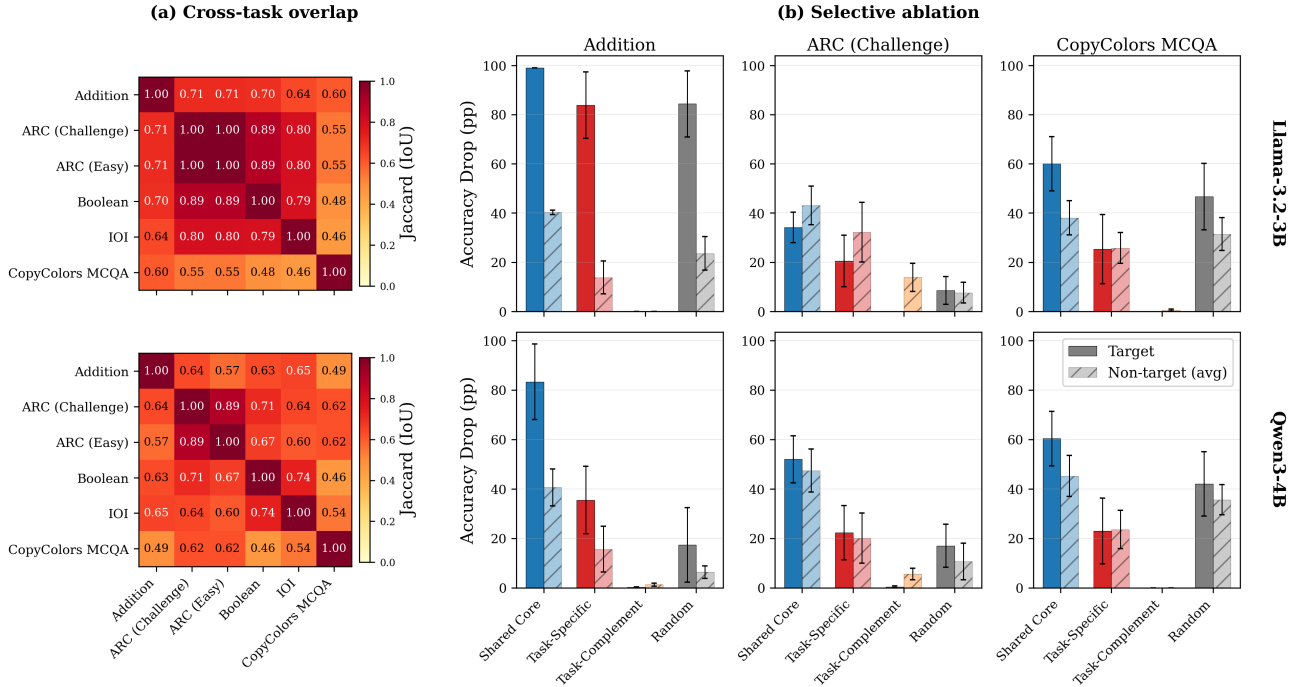


Figure 5. **Cross-task overlap and targeted removal at $K=10\%$.** (a) Overlap between task pairs’ circuits; high overlap explains why removing one task’s circuit damages other tasks comparably. (b) Accuracy drop from removing each circuit group: shared core, task-specific, complementary, and a random control of equal size. Solid bars show the target task drop; hatched bars show the mean drop on other tasks. Results shown for Llama-3.2-3B (top) and Qwen3-4B (bottom); see §F and §I for all K values and models.

circuit and most of the performance impact when removed. The task-specific components are a small portion of each circuit, but removing them does hurt the target task more than other tasks. Because the shared core dominates, removing any task’s circuit strips away roughly the same components and causes roughly the same performance degradation regardless of which task is being evaluated.

6. Discussion

6.1. Why do circuits overlap?

We hypothesize several (non-mutually-exclusive) explanations for high cross-task overlap.

MLP layers as shared infrastructure. At small circuit sizes, circuits are composed almost entirely of MLP layers (§K). This likely contributes to the especially high overlap at small K : because models have far fewer MLP layers than attention heads, MLP-dominated circuits are constrained to draw from a small shared set of components. Beyond this, these layers plausibly perform general-purpose operations – storing parametric knowledge (Sun et al., 2025; Liu et al., 2025), mapping tokens into a useful representational space, adjusting positional information – that all downstream computation depends on, regardless of task. Indeed, activation steering typically operates on post-MLP

residual stream states (Subramani et al., 2022) rather than individual attention heads.

Polysemanticity and superposition. The observation by Elhage et al. (2022) that neural networks represent more features than they have dimensions implies that individual heads and MLP layers inevitably serve multiple roles. At the granularity of entire MLP layers, these roles cannot be disentangled, so circuits for different tasks will overlap even if the underlying feature-level computations are distinct. A natural response is to move to finer-grained units of analysis: Marks et al. (2025) propose sparse feature circuits built on sparse autoencoders, which decompose polysemantic components into monosemantic features and may recover the task-specific structure that component-level analysis misses. Whether feature-level circuits exhibit greater specificity than what we observe here is a relevant open question.

Reuse as a feature, not a bug. Our framing so far has treated non-specificity as a limitation of circuit discovery, but this implicitly assumes that task circuits *ought* to be disjoint. It is worth noting that high reuse may itself be a desirable property. An alternative hypothesis holds that models develop (via training pressures) small, reusable computational motifs (*e.g.*, induction heads, copy-suppression heads) that function as general-purpose neural machinery - and that

finding these shared primitives is a valuable interpretability goal. Reuse is plausibly one driver of generalization: in-context learning, for example, likely succeeds precisely because models can apply the same retrieval and binding operations across novel tasks without dedicated machinery for each. Here, the shared core is not a confounder, but a meaningful object of study in its own right.

6.2. What does this mean for circuit-level analysis?

The value proposition of per-task circuit discovery implicitly relies on specificity: if task A 's circuit largely matches task B 's, identifying A 's circuit reveals more about what the model needs to function at all than about how it specifically performs A . Our results suggest this is the more accurate description at the granularity of attention heads and MLP layers - though the selective ablation experiments do reveal a smaller set of task-specific components embedded within this shared core, particularly for Addition.

Recovering task-specific structure reliably may require either (a) finer-grained units of analysis, such as sparse feature circuits (Marks et al., 2025), or (b) attribution methods that explicitly control for shared infrastructure - for example, by identifying components with high attribution for one task *relative to* others, rather than in absolute terms.

6.3. Broader implications

The broad reuse of causally important MLP layers has implications beyond circuit analysis. Model editing methods (Meng et al., 2022; Dai et al., 2022) modify specific weight matrices to target specific factual associations, but if those matrices are load-bearing across many tasks, targeted edits will produce wider effects than intended. This is consistent with existing evidence that localization does not straightforwardly inform editing (Hase et al., 2023) and that editing techniques suffer from low specificity (Hoelscher-Obermaier et al., 2023). Safety interventions present a somewhat different picture, as they typically steer directions within activation space rather than ablating entire components (Li et al., 2023), and our results therefore apply less directly. The broader lesson is that the degree of modularity depends heavily on the granularity of analysis, and conclusions drawn at one level of description should not be assumed to hold at others.

7. Related Work

Circuit discovery and evaluation. One of the first works to almost fully reverse-engineer a model behavior was Wang et al. (2023), who identified a circuit for indirect object identification (IOI) in GPT-2 Small. Subsequent work has scaled circuit discovery through automation: ACDC (Conmy et al., 2023), EAP (Syed et al., 2024), and relevance patching (Ja-

fari et al., 2025). We use EAP throughout for its scalability. On the evaluation side, Shi et al. (2024) propose statistical tests for necessity, sufficiency, and minimality. Miller et al. (2024) show that standard evaluation metrics can be fragile, and Hanna et al. (2024) introduce EAP-IG and argue that circuits should be evaluated by faithfulness rather than overlap with known circuits. Our work adds *consistency* and *specificity* to this evaluation toolkit.

Circuit reuse across tasks. The most closely related work is Merullo et al. (2024), who compare the IOI circuit to a Colored Objects circuit (BIG-bench authors, 2023) in GPT-2 Medium, finding 78% overlap in attention heads. They interpret this as evidence that models reuse algorithmic building blocks across tasks with a common underlying structure (both tasks require copying a token from context). Our work differs in scope, scale, and interpretation. We study six diverse tasks across seven models from four families, and find comparable overlap between tasks with no obvious shared algorithmic structure (e.g., Addition and ARC), driven by shared MLP layers rather than shared algorithmic roles. This suggests that component-level overlap may largely reflect dependence on general-purpose infrastructure - a distinction hard to make when comparing algorithmically similar tasks. Notably, our CopyColors MCQA task (Mueller et al., 2025) is similar in spirit to their Colored Objects task, yet shows comparable overlap with unrelated tasks like Addition.

8. Conclusion

We evaluated two underexplored properties of language model circuits - consistency (whether the same components recur across inputs to a task) and specificity (whether circuits are unique to their task). Across six tasks and seven models, we find that circuits are consistent - shared components appear reliably and prove causally necessary - but are largely not specific: circuits for different tasks overlap extensively and ablating one task's circuit damages others comparably. Both of these are explained by a heavy reliance on shared MLP-layers.

What should the field take from this? We think the primary lesson is that, at the level of attention heads and MLP layers, circuit discovery is effective at identifying which components are important (consistency), but most of the identified components are important for *everything*, not just the target task (non-specificity). A smaller set of task-specific components does exist within some circuits and shows selective causal effects - but these are a minority, embedded in a much larger shared core. Whether existing or new circuit discovery methods can reliably isolate this task-specific signal - through finer-grained methods like sparse feature circuits (Marks et al., 2025), contrastive attribution, or other approaches - remains an important open question.

9. Acknowledgments

We thank Arnab Sen Sharma and other members of the Bau Lab for their helpful discussions. We are also grateful to Tanush Chopra for valuable feedback on early drafts of this work, and to the anonymous reviewers for their thoughtful comments and suggestions, particularly their recommendation to conduct cross-task experiments, which greatly improved the paper.

References

- Ameisen, E., Lindsey, J., Pearce, A., Gurnee, W., Turner, N. L., Chen, B., Citro, C., Abrahams, D., Carter, S., Hosmer, B., Marcus, J., Sklar, M., Templeton, A., Bricken, T., McDougall, C., Cunningham, H., Henighan, T., Jermyn, A., Jones, A., Persic, A., Qi, Z., Ben Thompson, T., Zimmerman, S., Rivoire, K., Conerly, T., Olah, C., and Batson, J. Circuit tracing: Revealing computational graphs in language models. *Transformer Circuits Thread*, 2025. URL <https://transformer-circuits.pub/2025/attribution-graphs/methods.html>.
- Arora, A., Wu, Z., Steinhardt, J., and Schwettmann, S. Language model circuits are sparse in the neuron basis. <https://transluce.org/neuron-circuits>, November 2025.
- Clark, P., Cowhey, I., Etzioni, O., Khot, T., Sabharwal, A., Schoenick, C., and Tafford, O. Think you have solved question answering? try arc, the ai2 reasoning challenge. *ArXiv*, abs/1803.05457, 2018. URL <https://api.semanticscholar.org/CorpusID:3922816>.
- Conmy, A., Mavor-Parker, A., Lynch, A., Heimersheim, S., and Garriga-Alonso, A. Towards automated circuit discovery for mechanistic interpretability. In Oh, A., Naumann, T., Globerson, A., Saenko, K., Hardt, M., and Levine, S. (eds.), *Advances in Neural Information Processing Systems*, volume 36, pp. 16318–16352. Curran Associates, Inc., 2023. URL https://proceedings.neurips.cc/paper_files/paper/2023/file/34e1dbe95d34d7ebaf99b9bcaeb5b2be-Paper-Conference.pdf.
- Dai, D., Dong, L., Hao, Y., Sui, Z., Chang, B., and Wei, F. Knowledge neurons in pretrained transformers. In *Proceedings of the 60th Annual Meeting of the Association for Computational Linguistics*, 2022.
- Elhage, N., Nanda, N., Olsson, C., Henighan, T., Joseph, N., Mann, B., Askell, A., Bai, Y., Chen, A., Conerly, T., DasSarma, N., Drain, D., Ganguli, D., Hatfield-Dodds, Z., Hernandez, D., Jones, A., Kernion, J., Lovitt, L., Ndousse, K., Amodei, D., Brown, T., Clark, J., Kaplan, J., McCandlish, S., and Olah, C. A mathematical framework for transformer circuits. *Transformer Circuits Thread*, 2021. URL <https://transformer-circuits.pub/2021/framework/index.html>.
- Elhage, N., Hume, T., Olsson, C., Schiefer, N., Henighan, T., Kravec, S., Hatfield-Dodds, Z., Lasenby, R., Drain, D., Chen, C., Grosse, R., McCandlish, S., Kaplan, J., Amodei, D., Wattenberg, M., and Olah, C. Toy models of superposition. *Transformer Circuits Thread*, 2022. URL https://transformer-circuits.pub/2022/to_model/index.html.
- Gemma Team. Gemma 2: Improving open language models at a practical size. 2024. URL <https://arxiv.org/abs/2408.00118>.
- Hanna, M., Pezzelle, S., and Belinkov, Y. Have faith in faithfulness: Going beyond circuit overlap when finding model mechanisms. In *ICML 2024 Workshop on Mechanistic Interpretability*, 2024. URL <https://openreview.net/forum?id=grXgesr5dT>.
- Hase, P., Bansal, M., Kim, B., and Ghandeharioun, A. Does localization inform editing? surprising differences in causality-based localization vs. knowledge editing in language models. In *Thirty-seventh Conference on Neural Information Processing Systems*, 2023. URL <https://openreview.net/forum?id=ElDbULZtbd>.
- Hoelscher-Obermaier, J., Persson, J., Kran, E., Konstas, I., and Barez, F. Detecting edit failures in large language models: An improved specificity benchmark. In Rogers, A., Boyd-Graber, J., and Okazaki, N. (eds.), *Findings of the Association for Computational Linguistics: ACL 2023*, pp. 11548–11559, Toronto, Canada, July 2023. Association for Computational Linguistics. doi: 10.18653/v1/2023.findings-acl.733. URL <https://aclanthology.org/2023.findings-acl.733/>.
- Jafari, F. R., Eberle, O., Khakzar, A., and Nanda, N. Relp: Faithful and efficient circuit discovery via relevance patching. In *Mechanistic Interpretability Workshop at NeurIPS 2025*, 2025. URL <https://openreview.net/forum?id=5PKPy82sWN>.
- Li, K., Patel, O., Viégas, F., Pfister, H., and Wattenberg, M. Inference-time intervention: Eliciting truthful answers from a language model. In *Advances in Neural Information Processing Systems*, 2023.
- Liu, J., Jain, J., Diab, M., and Subramani, N. Llm microscope: What model internals reveal about answer correctness and context utilization. *arXiv preprint arXiv:2510.04013*, 2025.
- Llama team. The llama 3 herd of models. 2024. URL <https://arxiv.org/abs/2407.21783>.

- Marks, S., Rager, C., Michaud, E. J., Belinkov, Y., Bau, D., and Mueller, A. Sparse feature circuits: Discovering and editing interpretable causal graphs in language models. In *The Thirteenth International Conference on Learning Representations*, 2025. URL <https://openreview.net/forum?id=I4e82CIDxv>.
- Meng, K., Bau, D., Andonian, A., and Belinkov, Y. Locating and editing factual associations in GPT. In *Advances in Neural Information Processing Systems*, 2022. URL <https://openreview.net/forum?id=-h6WAS6eE4>.
- Merullo, J., Eickhoff, C., and Pavlick, E. Circuit component reuse across tasks in transformer language models. In *The Twelfth International Conference on Learning Representations*, 2024. URL <https://openreview.net/forum?id=fpoAYV6Wsk>.
- Miller, J., Chughtai, B., and Saunders, W. Transformer circuit evaluation metrics are not robust. In *First Conference on Language Modeling*, 2024. URL <https://openreview.net/forum?id=zSf8PJyQb2>.
- Mueller, A., Geiger, A., Wiegrefe, S., Arad, D., Arcuschin, I., Belfki, A., Chan, Y. S., Fiotto-Kaufman, J. F., Haklay, T., Hanna, M., Huang, J., Gupta, R., Nikankin, Y., Orgad, H., Prakash, N., Reusch, A., Sankaranarayanan, A., Shao, S., Stolfo, A., Tutek, M., Zur, A., Bau, D., and Belinkov, Y. MIB: A mechanistic interpretability benchmark. In *Forty-second International Conference on Machine Learning*, 2025. URL <https://openreview.net/forum?id=sSr0wve6vb>.
- Pearl, J. Causal diagrams for empirical research. *Biometrika*, 82(4):669–688, 1995. ISSN 00063444, 14643510. URL <http://www.jstor.org/stable/2337329>.
- Shi, C., Beltran-Velez, N., Nazaret, A., Zheng, C., Garriga-Alonso, A., Jesson, A., Makar, M., and Blei, D. Hypothesis testing the circuit hypothesis in LLMs. In *The Thirty-eighth Annual Conference on Neural Information Processing Systems*, 2024. URL <https://openreview.net/forum?id=5ai2YFAXV7>.
- Subramani, N., Suresh, N., and Peters, M. Extracting latent steering vectors from pretrained language models. In Muresan, S., Nakov, P., and Villavicencio, A. (eds.), *Findings of the Association for Computational Linguistics: ACL 2022*, pp. 566–581, Dublin, Ireland, May 2022. Association for Computational Linguistics. doi: 10.18653/v1/2022.findings-acl.48. URL <https://aclanthology.org/2022.findings-acl.48/>.
- Sun, Z., Zang, X., Zheng, K., Xu, J., Zhang, X., Yu, W., Song, Y., and Li, H. RedeEP: Detecting hallucination in retrieval-augmented generation via mechanistic interpretability. In *The Thirteenth International Conference on Learning Representations*, 2025. URL <https://openreview.net/forum?id=ztzZDzgrfh>.
- Syed, A., Rager, C., and Conmy, A. Attribution patching outperforms automated circuit discovery. In Belinkov, Y., Kim, N., Jumelet, J., Mohebbi, H., Mueller, A., and Chen, H. (eds.), *Proceedings of the 7th BlackboxNLP Workshop: Analyzing and Interpreting Neural Networks for NLP*, pp. 407–416, Miami, Florida, US, November 2024. Association for Computational Linguistics. doi: 10.18653/v1/2024.blackboxnlp-1.25. URL <https://aclanthology.org/2024.blackboxnlp-1.25/>.
- Team OLMo. 2 OLMo 2 Furious. 2024. URL <https://arxiv.org/abs/2501.00656>.
- Tenney, I., Das, D., and Pavlick, E. BERT rediscovers the classical NLP pipeline. In *Association for Computational Linguistics*, 2019. URL <https://arxiv.org/abs/1905.05950>.
- BIG-bench authors. Beyond the imitation game: Quantifying and extrapolating the capabilities of language models. *Transactions on Machine Learning Research*, 2023. ISSN 2835-8856. URL <https://openreview.net/forum?id=uyTL5Bvosj>.
- Vig, J., Gehrmann, S., Belinkov, Y., Qian, S., Nevo, D., Singer, Y., and Shieber, S. Investigating gender bias in language models using causal mediation analysis. In Larochelle, H., Ranzato, M., Hadsell, R., Balcan, M., and Lin, H. (eds.), *Advances in Neural Information Processing Systems*, volume 33, pp. 12388–12401. Curran Associates, Inc., 2020. URL https://proceedings.neurips.cc/paper_files/paper/2020/file/92650b2e92217715fe312e6fa7b90d82-Paper.pdf.
- Wang, K. R., Variengien, A., Conmy, A., Shlegeris, B., and Steinhardt, J. Interpretability in the wild: a circuit for indirect object identification in GPT-2 small. In *The Eleventh International Conference on Learning Representations*, 2023. URL <https://openreview.net/forum?id=NpsVSN6o4ul>.
- Yang, A., Li, A., Yang, B., Zhang, B., Hui, B., Zheng, B., Yu, B., Gao, C., Huang, C., Lv, C., Zheng, C., Liu, D., Zhou, F., Huang, F., Hu, F., Ge, H., Wei, H., Lin, H., Tang, J., Yang, J., Tu, J., Zhang, J., Yang, J., Yang, J., Zhou, J., Zhou, J., Lin, J., Dang, K., Bao, K., Yang, K., Yu, L., Deng, L., Li, M., Xue, M., Li, M., Zhang, P., Wang, P., Zhu, Q., Men, R., Gao, R., Liu, S., Luo, S., Li, T., Tang, T., Yin, W., Ren, X., Wang, X., Zhang, X., Ren, X., Fan, Y., Su, Y., Zhang, Y., Zhang, Y., Wan, Y., Liu, Y., Wang, Z., Cui, Z., Zhang, Z., Zhou, Z., and Qiu, Z. Qwen3 technical report. *arXiv preprint arXiv:2505.09388*, 2025.

A. Limitations

Our analysis uses a single circuit extraction method (EAP) and operates at the granularity of attention heads and MLP layers. While Syed et al. (2024) show that EAP recovers circuits competitive with those found by more expensive methods, we cannot rule out that different circuit extraction methods would yield different specificity patterns. Relatedly, we cannot rule out that gradient-based attribution is simply biased toward components with large activation magnitudes, which could inflate apparent overlap. However, our causal ablation experiments confirm that the shared components are functionally important (positive necessity), rather than merely high-scoring artifacts of the attribution method. Testing whether alternative extraction methods (e.g., relevance propagation) recover greater task specificity is an important direction for future work.

Different granularities (e.g., individual neurons, sparse autoencoder features) might also yield qualitatively different conclusions about specificity. Additionally, the small number of MLP layers relative to attention heads means that MLP-heavy circuits are structurally constrained to overlap; our results should be interpreted with this prior in mind. Our tasks, while diverse, do not include generative or multi-step tasks; it is possible that more complex tasks would show different patterns of reuse. Finally, our models range from 1B to 8B parameters. Scaling behavior at larger model sizes remains an open question.

B. Edge Attribution Patching Details

Given a clean input x and a corrupted input x' , EAP computes the attribution score for each component u as a first-order approximation of the effect of patching that component’s activation:

$$\hat{e}_u = (a_u(x') - a_u(x))^\top \cdot \frac{\partial L(x)}{\partial a_u}$$

where $a_u(\cdot)$ denotes the activation of component u and $L(x)$ is a scalar metric (e.g., logit difference) evaluated on the clean input. The score is the dot product of the activation difference between corrupt and clean inputs with the gradient of the metric with respect to that activation, summed over sequence positions. In practice, this is just a single line of PyTorch code:

```
score = (act_corrupt - act_clean) * grad
```

where `act_corrupt` and `act_clean` are the component’s activations under the corrupted and clean inputs respectively, and `grad` is the gradient of the metric with respect to the clean activation. Per-component scores are obtained by summing over positions and (for attention heads) the head dimension.

C. Task Details

Activation patching and its approximations require a clean input x and a corrupted input x' that alters the information the model must use while preserving surface structure as much as possible. The attribution metric for all tasks is the logit difference between the correct and incorrect answer tokens. Below we describe each task and its corruption strategy.

Addition. The model is given a 2-digit arithmetic problem (e.g., “Compute: $47 + 63 =$ ”) and must produce the correct sum. Corrupted inputs are generated by pairing each problem with a randomly selected different problem from the same batch, so the corrupted input has the same format but different operands and a different answer.

Boolean Logic. The model evaluates logical expressions composed of `and`, `or`, and `not` over boolean literals (e.g., “Evaluate: `true and (false or true) =`” \rightarrow “`true`”). Corrupted inputs are produced by randomly flipping one boolean literal in the expression (e.g., `true` \rightarrow `false`), which changes the expression’s truth value while preserving its syntactic structure.

Indirect Object Identification (IOI). Following the task setup in Wang et al. (2023), the model must identify the indirect object in sentences with a specific template involving two names (e.g., “Bilbo and Frodo spoke in Rivendell before Bilbo gave Sting to” \rightarrow “Frodo”). We use the dataset and counterfactuals from the Mechanistic Interpretability Benchmark (Mueller et al., 2025). The corrupted input applies the S2-IO flip counterfactual, which swaps the subject and indirect object names so that the correct completion changes while the sentence template remains identical.

CopyColors MCQA. A multiple-choice task from Mueller et al. (2025) in which the model is given a passage describing objects and their colors, followed by a question asking which color corresponds to a particular object. The answer choices are presented as labeled options (A, B, C, D). The corrupted input applies the answer-position counterfactual from the benchmark, which permutes the order of the answer choices so that the correct answer appears at a different position, changing the correct label token while keeping the passage and question unchanged.

ARC Easy / ARC Challenge. The AI2 Reasoning Challenge (Clark et al., 2018) consists of multiple-choice science exam questions. The Easy split contains questions answerable with basic retrieval and reasoning, while the Challenge split filters for questions requiring more complex inference. We use the datasets and counterfactuals from Mueller et al. (2025). As with CopyColors MCQA, the corrupted input

Model	HuggingFace ID	Params	$ L $	$ a $	d_{model}
Gemma 2 2B	google/gemma-2-2b	2.6B	26	8	2304
Gemma 2 2B Instruct	google/gemma-2-2b-it	2.6B	26	8	2304
Llama-3.2-3B	meta-llama/Llama-3.2-3B	3.2B	28	24	3072
Llama-3.2-3B Instruct	meta-llama/Llama-3.2-3B-Instruct	3.2B	28	24	3072
Qwen3-4B	Qwen/Qwen3-4B	4.0B	36	32	2560
Qwen3-8B	Qwen/Qwen3-8B	8.2B	36	32	4096
OLMo-2-1B	allenai/OLMo-2-0425-1B	1.2B	16	16	2048

Table 2. **Models studied in this work.** We report the number of parameters, number of layers $|L|$, total number of attention heads $|a|$, and hidden dimension d_{model} for each model.

applies the answer-position counterfactual, permuting the order of answer choices so that the correct label changes.

D. Model Details

See Table 2 for a list of model information.

E. Full Within-Task Results

Table 3 reports reuse@ P for all models, tasks, and circuit sizes K , and Table 4 reports the corresponding necessity values.

F. Full Cross-Task Results

Table 5 reports own-circuit vs. other-circuit accuracy drops for all models and circuit sizes. Figure 6 shows the cross-task Jaccard overlap heatmaps across all values of K .

G. Circuit Composition Across Models

Table 6 reports the MLP and attention head fractions of each circuit across all models, tasks, and circuit sizes K .

H. Layer Distribution of Circuit Components

Figure 7 shows the cumulative fraction of circuit components across model depth for each task and circuit size K . In the Llama and Qwen families, the CDF at small K is shifted toward earlier layers, indicating that the highest-attribution components tend to sit in early-to-middle layers. The Gemma family is less uniform: for tasks like IOI and CopyColors MCQA, the small- K circuit is concentrated in middle-to-late layers rather than early ones. At larger K , the distribution becomes more uniform across layers in all models.

I. Selective Ablation Across K

Figure 8 and Figure 9 shows the selective ablation results for $K \in \{1, 5, 10, 20, 30\}\%$, complementing the $K=10\%$ results in the main text.

J. Circuit Decomposition Sizes

Table 7 shows the mean number of components in each partition (shared core / task-specific / task-complement) for all models and tasks.

At small K ($\leq 5\%$), the shared core is near-empty for the Gemma models, reflecting their low cross-task overlap at strict thresholds. For the Llama and Qwen families, the shared core already dominates at $K=5\%$, accounting for 73–78% of the decomposition on average. As K grows, the shared core’s absolute size increases across all models, but its relative share decreases: at $K=10\%$ it constitutes 45–67% of the decomposition, dropping to 40–60% at $K=30\%$. The task-specific and task-complement sets grow faster in both absolute and relative terms as more lower-attribution components enter the circuit. The larger Qwen models have substantially larger circuits in absolute terms (*e.g.*, 45 components at $K=10\%$ vs. 15 for Gemma), but the proportional breakdown is similar, suggesting that the dominance of shared infrastructure is not an artifact of model size.

K. Component Breakdown

Tables 8–13 report the MLP fraction of each circuit for all models and tasks, extending the summary in the main text to the full set of models.

L. Pretraining Dynamics Tables

We report per-checkpoint values for the pretraining dynamics analysis of §4, split by circuit size $K \in \{1, 5, 10, 20, 30\}\%$. Rows cover the 18 stage-1 checkpoints (0B–4001B tokens) plus two stage-2 anneal checkpoints

How Much Do Circuits Tell Us? Measuring the Consistency and Specificity of Language Model Circuits

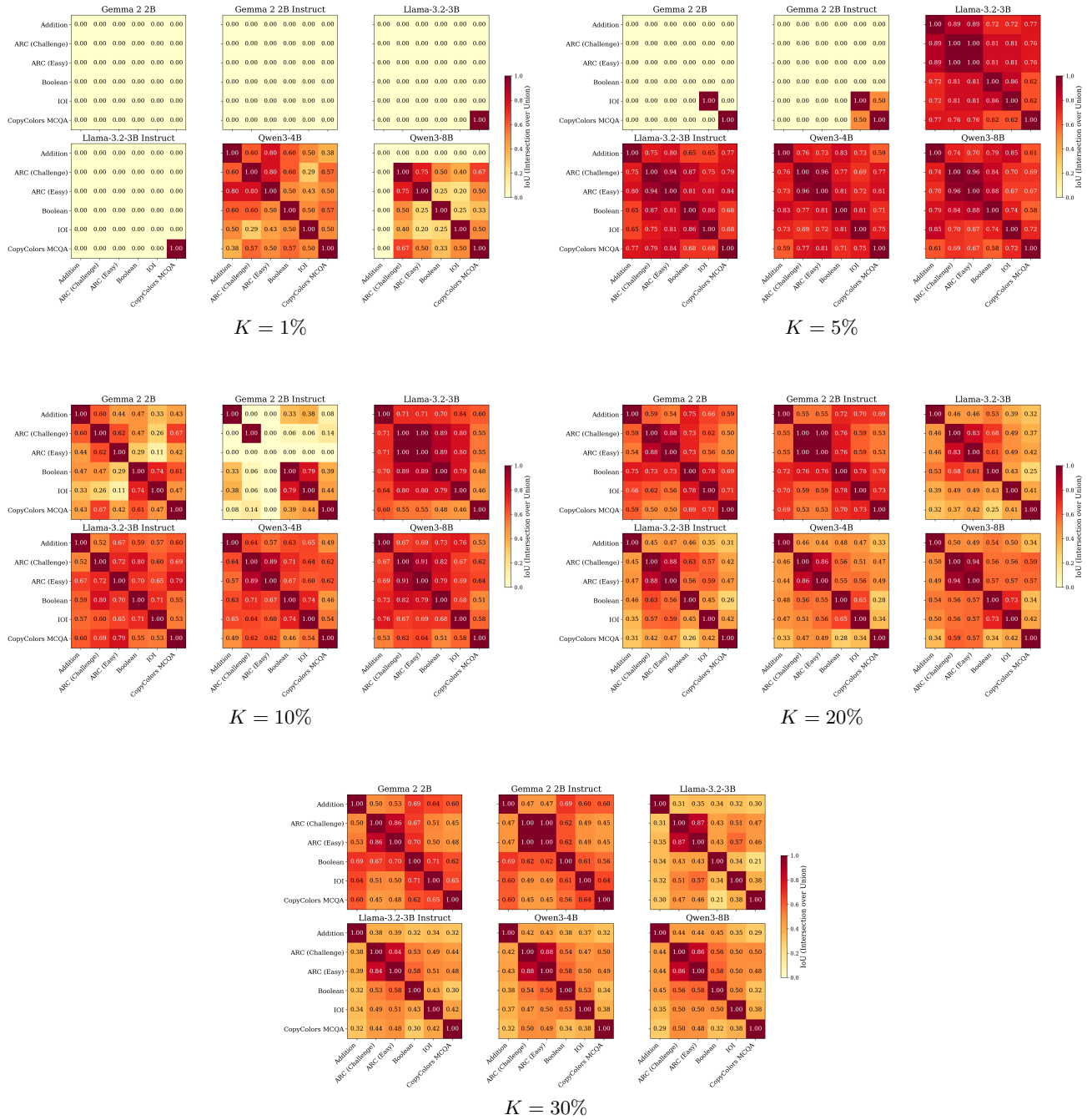


Figure 6. Cross-task Jaccard overlap across different values of K .

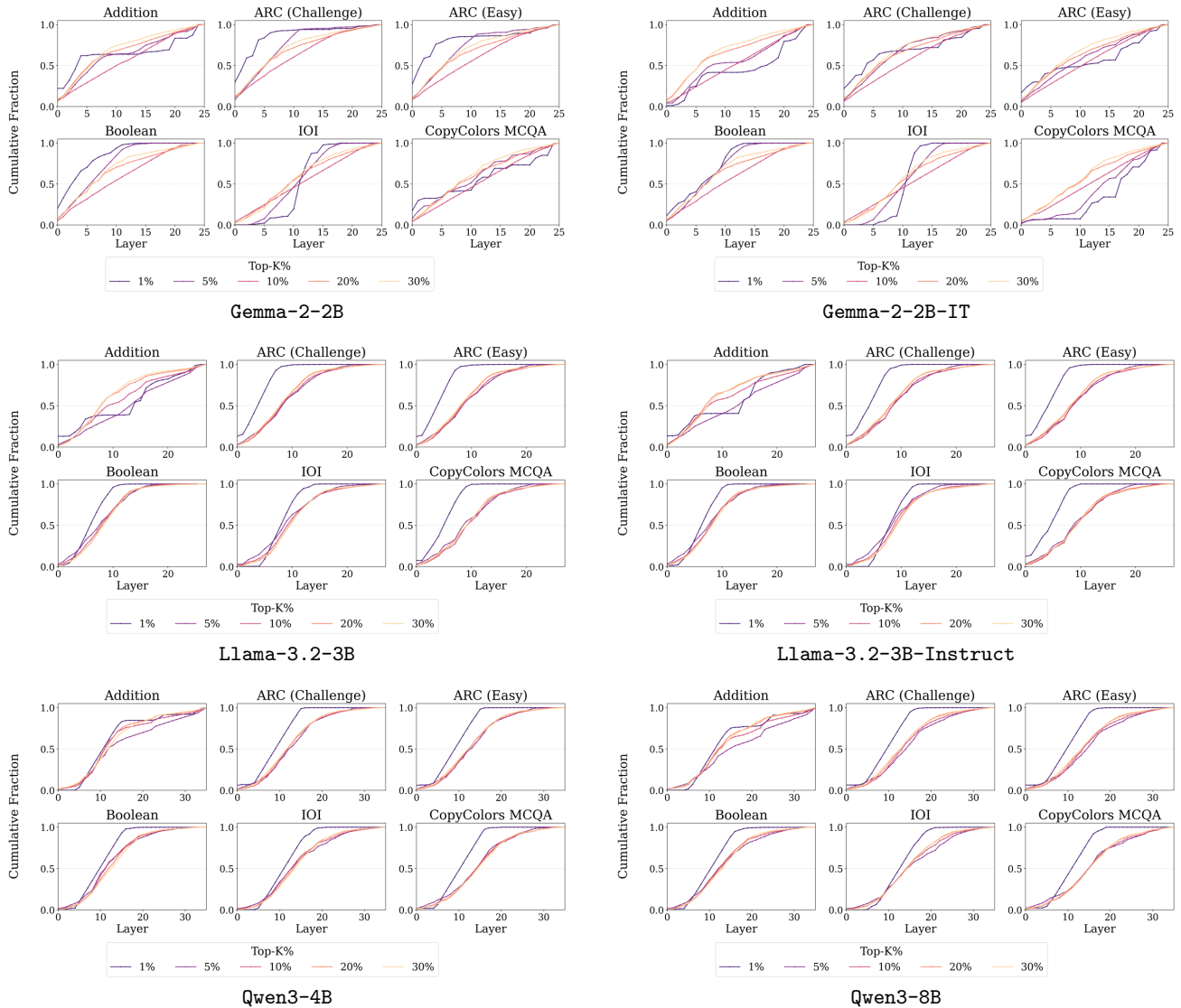


Figure 7. Cumulative layer distribution of circuit components. Each line shows the cumulative fraction of components in the top- $K\%$ circuit at or below a given layer. At small K , the CDF is shifted left (toward earlier layers) in the Llama and Qwen families but shows more task-dependent variation in the Gemma family.

How Much Do Circuits Tell Us? Measuring the Consistency and Specificity of Language Model Circuits

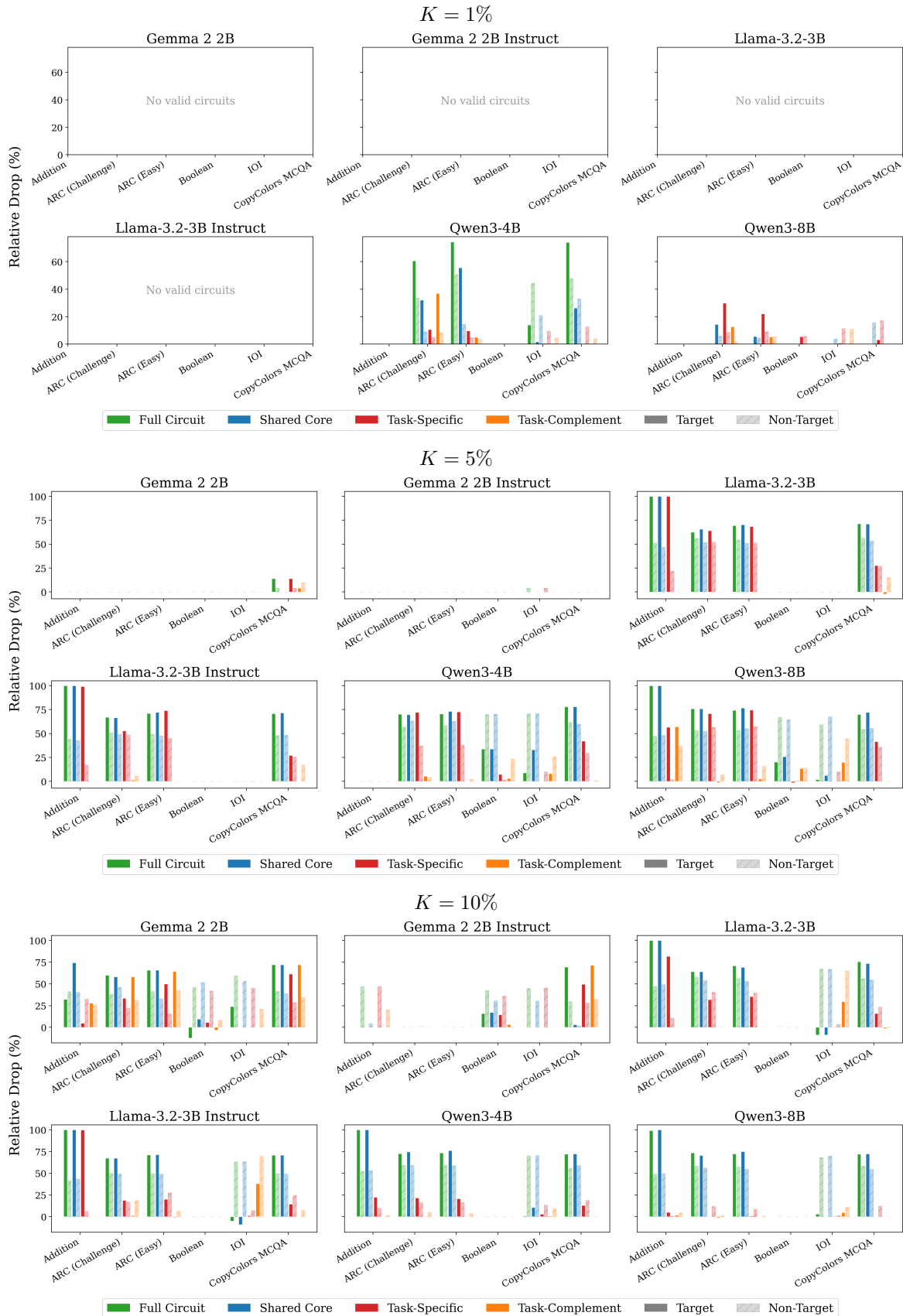


Figure 8. Selective ablation: relative accuracy drop by component set for $K \in \{1, 5, 10\}\%$.

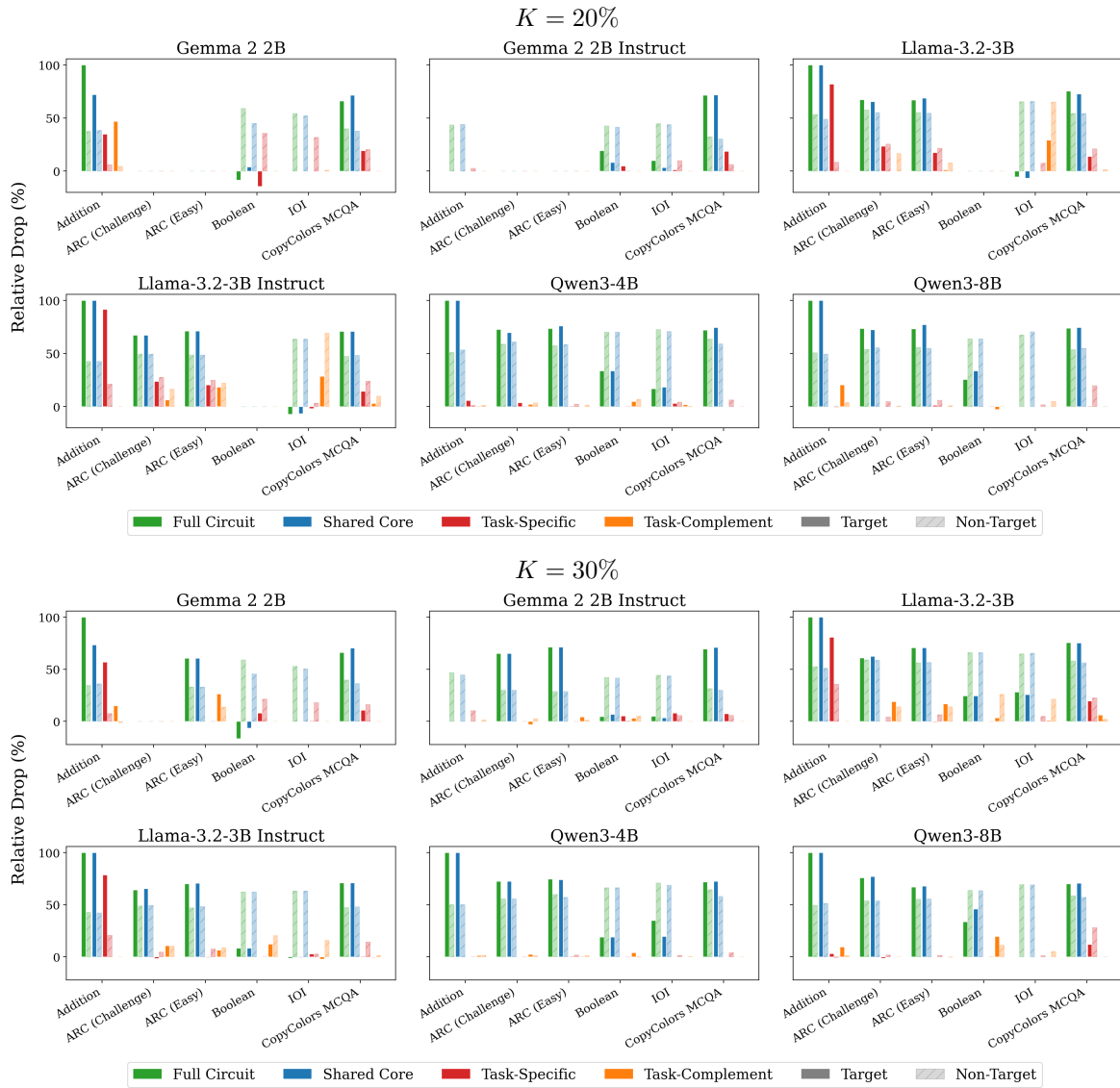


Figure 9. Selective ablation: relative accuracy drop by component set for $K \in \{20, 30\}\%$.

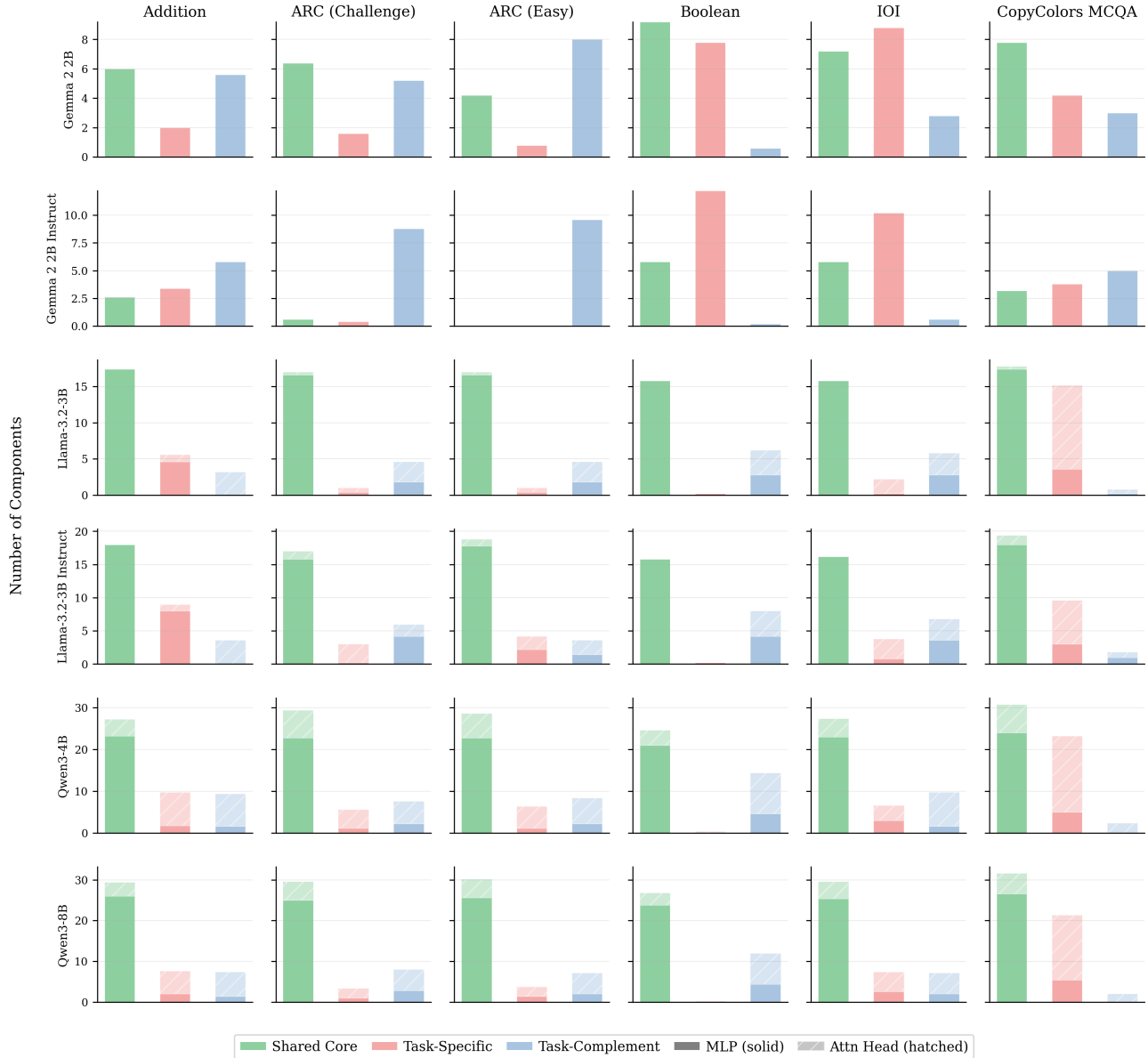


Figure 10. **MLP vs. attention head composition of circuit decompositions at $K=10\%$.** Each group of three bars shows the mean number of MLP layers (solid) and attention heads (hatched) in the shared core, task-specific, and task-complement sets. MLP layers account for the vast majority of the shared core across all models and tasks, while attention heads appear primarily in the task-specific and task-complement sets at larger circuit sizes.

K	Model	Addition	ARC (Challenge)	ARC (Easy)	Boolean	IOI	CopyColors	MCQA
1%	Gemma 2B	0	0	0	0	0		0
	Gemma 2B IT	0	0	0	0	0		0
	Llama 3B	0	0	14	29	43		14
	Llama 3B IT	0	0	0	43	43		14
	Qwen 4B	64	73	73	73	64		82
	Qwen 8B	27	64	64	64	64		73
5%	Gemma 2B	27	45	27	0	55		18
	Gemma 2B IT	9	0	0	0	64		9
	Llama 3B	80	49	49	46	49		63
	Llama 3B IT	80	51	54	46	46		57
	Qwen 4B	53	49	51	44	54		61
	Qwen 8B	54	54	54	42	56		64
10%	Gemma 2B	48	65	65	83	78		57
	Gemma 2B IT	70	61	48	83	87		48
	Llama 3B	49	34	36	24	37		51
	Llama 3B IT	49	39	41	26	43		46
	Qwen 4B	45	42	47	29	34		49
	Qwen 8B	42	38	42	30	35		49
20%	Gemma 2B	76	48	46	52	70		72
	Gemma 2B IT	78	39	41	50	70		70
	Llama 3B	44	34	35	22	41		54
	Llama 3B IT	45	36	38	23	48		56
	Qwen 4B	53	35	37	26	36		54
	Qwen 8B	45	36	38	27	34		51
30%	Gemma 2B	67	39	41	50	63		63
	Gemma 2B IT	70	39	39	44	64		63
	Llama 3B	50	40	40	31	43		58
	Llama 3B IT	60	42	43	36	52		57
	Qwen 4B	59	40	39	32	44		56
	Qwen 8B	50	36	36	30	41		53

Table 3. reuse@97 (%) across all circuit sizes K .

(anneal1, anneal3; each ~51B tokens of curated data with LR decay on top of stage-1).

Reuse tables. Tables 14–18 give reuse@95 (%) at each K . At $K = 1%$ (Table 14) circuits are tiny – often a single component – so reuse is 0 or 50% depending on whether that component is shared. At $K = 5%$ (Table 15) reuse fluctuates around 0–55% with no consistent trend. Table 16 corresponds to the top row of Figure 3: reuse starts near 50–60% in the first ~76B tokens and declines for the rest of stage-1, with Boolean’s $K = 10%$ shared circuit becoming empty from 399B onward. At $K = 20$ –30% (Tables 17 and 18) the shared circuit covers a larger fraction of the model, so per-checkpoint reuse is more stable (typically 25–40%).

Necessity tables. Tables 19–23 give necessity=(control – ablation)/baseline at each K , where ablation removes the reuse@95 shared circuit and control removes a capacity-matched random component set. A dash (–) marks checkpoints where baseline accuracy is 0 (ratio undefined); a 0.00 entry typically means the shared circuit is empty at

that K (no components in $\geq 95%$ of examples), making the ablation degenerate. Table 21 corresponds to the bottom row of Figure 3. The IOI columns are consistently negative across K , reflecting the anomaly noted in the main text: random ablation hurts more than shared-circuit ablation. At the anneal checkpoints, CopyColors MCQA shows the largest positive necessity at $K = 10$ –30% (e.g. baseline ~95% drops to 0% under shared-circuit ablation but only to 30% under random ablation), the only setting where the shared circuit is clearly causally distinguished from a capacity-matched random control.

K	Model	Addition	ARC (Challenge)	ARC (Easy)	Boolean	IOI	CopyColors	MCQA
1%	Gemma 2B	0.00	0.00	0.00	0.00	0.00		0.00
	Gemma 2B IT	–	0.00	0.00	0.00	0.00		0.00
	Llama 3B	0.00	0.00	0.18	0.05	0.02		0.00
	Llama 3B IT	0.00	0.00	0.00	0.36	0.08		0.11
	Qwen 4B	0.07	0.00	0.54	0.24	0.39		0.70
	Qwen 8B	-0.86	-0.01	0.62	0.05	0.08		-0.10
5%	Gemma 2B	0.29	0.07	-0.15	0.00	0.00		0.10
	Gemma 2B IT	–	0.00	0.00	0.00	-0.03		0.00
	Llama 3B	0.80	0.54	0.61	0.01	-0.16		0.70
	Llama 3B IT	0.44	0.58	0.61	-0.19	0.11		0.67
	Qwen 4B	0.04	0.00	0.00	0.00	0.00		0.70
	Qwen 8B	0.00	-0.04	0.56	0.24	0.01		0.40
10%	Gemma 2B	-0.68	0.00	0.00	-0.01	0.05		0.00
	Gemma 2B IT	–	0.51	0.40	0.04	-0.04		0.70
	Llama 3B	0.93	0.52	0.67	0.09	0.04		0.50
	Llama 3B IT	0.77	0.63	0.64	-0.24	-0.02		0.67
	Qwen 4B	0.99	0.04	0.64	0.34	0.00		0.70
	Qwen 8B	0.36	0.54	0.43	-0.01	-0.02		1.00
20%	Gemma 2B	1.01	0.01	0.07	0.02	0.21		0.70
	Gemma 2B IT	–	0.34	0.39	0.13	0.62		0.70
	Llama 3B	0.89	0.63	0.67	0.07	0.47		0.50
	Llama 3B IT	0.92	0.57	0.71	-0.10	0.32		0.56
	Qwen 4B	0.99	0.36	0.48	0.07	0.02		0.70
	Qwen 8B	0.98	0.76	0.71	0.13	0.02		0.70
30%	Gemma 2B	0.07	0.04	0.17	0.21	0.19		0.50
	Gemma 2B IT	–	0.32	0.48	0.34	0.09		0.70
	Llama 3B	0.94	0.53	0.64	0.35	0.38		0.70
	Llama 3B IT	0.77	0.54	0.66	-0.01	0.51		0.67
	Qwen 4B	0.93	0.67	0.70	0.37	-0.05		0.70
	Qwen 8B	0.98	0.68	0.69	0.18	0.00		1.00

Table 4. Necessity across all circuit sizes K .

K	Model	Addition	ARC (Challenge)	ARC (Easy)	Boolean	IOI	CopyColors MCQA
		Own/Oth.	Own/Oth.	Own/Oth.	Own/Oth.	Own/Oth.	Own/Oth.
1%	Gemma 2B	0/0	0/0	0/0	0/0	0/0	0/0
	Gemma 2B IT	0/0	0/0	0/0	0/0	0/0	0/0
	Llama 3B	0/0	0/0	0/0	0/0	0/0	0/0
	Llama 3B IT	0/0	0/0	0/0	0/0	0/0	0/0
	Qwen 4B	0/1	0/5	0/6	0/1	0/0	0/0
	Qwen 8B	0/0	0/0	0/0	0/0	0/0	0/0
5%	Gemma 2B	0/0	0/0	0/0	0/0	0/0	0/0
	Gemma 2B IT	0/0	0/0	0/0	0/0	0/0	0/0
	Llama 3B	99/99	41/41	56/57	18/18	-6/-3	66/70
	Llama 3B IT	100/100	47/47	64/66	14/6	11/-1	68/70
	Qwen 4B	100/100	57/58	75/74	13/21	37/6	76/72
	Qwen 8B	100/93	66/63	72/73	15/14	2/1	70/75
10%	Gemma 2B	-9/24	25/20	4/37	4/0	0/0	68/42
	Gemma 2B IT	0/-15	0/16	0/27	17/5	1/0	0/28
	Llama 3B	99/99	40/41	57/57	18/18	-5/12	70/68
	Llama 3B IT	100/100	47/47	64/65	1/4	-7/-3	68/68
	Qwen 4B	100/100	60/60	72/70	22/14	14/11	72/73
	Qwen 8B	99/100	64/64	70/70	19/26	3/1	72/76
20%	Gemma 2B	87/62	31/32	50/50	-6/-4	0/0	66/72
	Gemma 2B IT	0/-3	43/43	65/66	5/10	3/2	68/70
	Llama 3B	99/99	41/40	58/56	18/18	2/15	76/70
	Llama 3B IT	100/100	47/47	64/65	-2/5	-12/-3	68/68
	Qwen 4B	100/100	61/58	72/73	23/24	1/15	72/74
	Qwen 8B	100/100	64/60	71/74	19/20	0/1	74/73
30%	Gemma 2B	87/68	32/32	50/50	-6/-4	0/0	72/72
	Gemma 2B IT	0/-2	43/43	65/66	-7/15	9/4	68/70
	Llama 3B	99/99	41/38	57/57	18/18	-5/22	74/70
	Llama 3B IT	100/100	47/47	64/65	15/5	-4/-3	68/68
	Qwen 4B	100/100	61/63	73/74	23/24	17/21	72/75
	Qwen 8B	100/100	66/62	65/72	25/19	0/5	70/75

Table 5. Own-circuit vs. other-circuit accuracy drop (pp) across all K values. Each cell reports *Own/Oth.*, where Own is the drop from ablating that task’s circuit and Oth. is the mean drop from ablating other tasks’ circuits.

How Much Do Circuits Tell Us? Measuring the Consistency and Specificity of Language Model Circuits

K	Model	Addition	ARC (Challenge)	ARC (Easy)	Boolean	IOI	CopyColors MCQA
1%	Gemma 2B	-	-	-	-	-	-
	Gemma 2B IT	-	-	-	-	-	-
	Llama 3B	-	-	-	-	-	100/0
	Llama 3B IT	-	-	-	-	-	100/0
	Qwen 4B	100/0	100/0	100/0	100/0	100/0	100/0
	Qwen 8B	-	100/0	100/0	100/0	100/0	100/0
5%	Gemma 2B	-	-	-	-	100/0	100/0
	Gemma 2B IT	-	-	-	-	100/0	100/0
	Llama 3B	100/0	100/0	100/0	100/0	100/0	81/19
	Llama 3B IT	100/0	100/0	100/0	100/0	100/0	89/11
	Qwen 4B	90/10	88/12	88/12	91/9	88/12	77/23
	Qwen 8B	100/0	92/8	92/8	95/5	88/12	78/22
10%	Gemma 2B	100/0	100/0	100/0	100/0	100/0	100/0
	Gemma 2B IT	100/0	100/0	-	100/0	100/0	100/0
	Llama 3B	96/4	94/6	94/6	100/0	89/11	64/36
	Llama 3B IT	96/4	80/20	87/13	100/0	85/15	72/28
	Qwen 4B	68/32	69/31	69/31	84/16	76/24	54/46
	Qwen 8B	76/24	79/21	79/21	89/11	76/24	60/40
20%	Gemma 2B	78/22	100/0	94/6	95/5	92/8	78/22
	Gemma 2B IT	79/21	100/0	100/0	100/0	89/11	80/20
	Llama 3B	78/22	72/28	68/32	100/0	53/47	36/64
	Llama 3B IT	71/29	67/33	65/35	95/5	49/51	35/65
	Qwen 4B	39/61	43/57	47/53	65/35	66/34	26/74
	Qwen 8B	48/52	48/52	50/50	75/25	64/36	33/67
30%	Gemma 2B	69/31	89/11	80/20	85/15	74/26	60/40
	Gemma 2B IT	69/31	89/11	89/11	92/8	74/26	62/38
	Llama 3B	47/53	40/60	43/57	72/28	39/61	23/77
	Llama 3B IT	39/61	46/54	45/55	59/41	33/67	24/76
	Qwen 4B	22/78	32/68	34/66	49/51	39/61	19/81
	Qwen 8B	31/69	39/61	40/60	51/49	39/61	21/79

Table 6. Shared circuit composition across models and tasks. Entries are MLP/attention-head percentages.

K	Model	Addition	ARC (Challenge)	ARC (Easy)	Boolean	IOI	CopyColors MCQA
5%	Gemma 2B	0/0/1	0/0/1	0/0/1	0/0/1	0/1/0	0/2/0
	Gemma 2B IT	0/0/1	0/0/1	0/0/1	0/0/1	0/2/0	0/1/0
	Llama 3B	15/3/1	15/1/1	15/1/1	13/0/4	13/0/4	15/6/0
	Llama 3B IT	15/5/0	14/1/2	15/1/1	13/0/4	13/0/4	15/4/1
	Qwen 4B	19/1/6	21/3/3	22/3/2	21/1/4	21/4/3	23/8/0
	Qwen 8B	20/2/6	22/3/4	22/2/4	20/1/6	22/4/4	24/12/0
10%	Gemma 2B	6/2/6	6/2/5	4/1/8	9/8/1	7/9/3	8/4/3
	Gemma 2B IT	3/3/6	1/0/9	0/0/10	6/12/0	6/10/1	3/4/5
	Llama 3B	17/6/3	17/1/5	17/1/5	16/0/6	16/2/6	18/15/1
	Llama 3B IT	18/9/4	17/3/6	19/4/4	16/0/8	16/4/7	19/10/2
	Qwen 4B	27/10/9	29/6/8	29/6/8	25/0/14	27/7/10	31/23/2
	Qwen 8B	29/8/7	30/3/8	30/4/7	27/0/12	30/7/7	32/21/2
20%	Gemma 2B	19/8/3	16/0/9	15/1/9	19/3/4	19/7/3	20/12/1
	Gemma 2B IT	20/9/2	16/0/9	16/0/9	19/2/5	20/7/2	20/10/2
	Llama 3B	19/13/15	21/4/15	22/6/14	17/0/21	21/15/13	25/42/3
	Llama 3B IT	22/16/17	25/5/15	27/7/13	19/0/24	25/14/14	28/44/4
	Qwen 4B	40/31/24	45/15/22	45/14/22	34/3/37	37/7/33	48/73/6
	Qwen 8B	38/20/24	47/15/14	46/14/15	35/1/31	38/9/25	48/55/5

Table 7. Mean circuit decomposition sizes across K values, averaged over task-pair partners. Each cell shows Shared/Specific/Complement counts ($|C_A \cap C_B|/|C_A \setminus C_B|/|C_B \setminus C_A|$).

Table 8. Gemma 2 2B: mean attention heads /MLPs in the top- K % circuit.

Task	1%	10%	20%	30%
Addition	0.0/3.0	1.0/23.0	21.6/25.4	45.4/25.6
ARC (Challenge)	0.0/3.0	3.5/20.5	23.5/23.5	46.5/24.5
ARC (Easy)	0.0/3.0	2.3/21.7	22.5/24.5	45.9/25.1
Boolean	0.0/3.0	2.1/21.9	22.7/24.3	46.2/24.8
IOI	0.0/3.0	0.1/23.9	21.4/25.6	45.2/25.8
CopyColors MCQA	0.0/3.0	0.1/23.9	21.2/25.8	45.1/25.9

Table 9. Gemma 2 2B Instruct: mean attention heads /MLPs in the top- K % circuit.

Task	1%	10%	20%	30%
Addition	0.0/3.0	0.1/23.9	21.3/25.7	45.2/25.8
ARC (Challenge)	0.0/3.0	1.6/22.4	22.4/24.6	45.9/25.1
ARC (Easy)	0.0/3.0	0.9/23.1	21.9/25.1	45.6/25.4
Boolean	0.0/3.0	1.6/22.4	22.3/24.7	45.9/25.1
IOI	0.0/3.0	0.1/23.9	21.4/25.6	45.3/25.7
CopyColors MCQA	0.0/3.0	0.3/23.7	21.2/25.8	45.1/25.9

Table 10. Llama-3.2-3B: mean attention heads /MLPs in the top- K % circuit.

Task	1%	10%	20%	30%
Addition	0.4/6.6	42.3/27.7	112.2/27.8	182.1/27.9
ARC (Challenge)	0.0/7.0	47.0/23.0	114.9/25.1	183.7/26.3
ARC (Easy)	0.0/7.0	46.5/23.5	114.4/25.6	183.5/26.5
Boolean	0.0/7.0	50.7/19.3	118.6/21.4	186.7/23.3
IOI	0.0/7.0	46.7/23.3	113.4/26.6	182.8/27.2
CopyColors MCQA	0.0/7.0	46.1/23.9	113.7/26.3	183.0/27.0

Table 11. Llama-3.2-3B Instruct: mean attention heads /MLPs in the top- K % circuit.

Task	1%	10%	20%	30%
Addition	0.5/6.5	42.3/27.7	112.2/27.8	182.1/27.9
ARC (Challenge)	0.0/7.0	45.7/24.3	113.5/26.5	182.9/27.1
ARC (Easy)	0.0/7.0	45.5/24.5	113.5/26.5	182.9/27.1
Boolean	0.1/6.9	49.5/20.5	116.9/23.1	184.8/25.2
IOI	0.0/7.0	48.4/21.6	113.5/26.5	182.8/27.2
CopyColors MCQA	0.0/7.0	45.4/24.6	113.5/26.5	182.9/27.1

Table 12. Qwen3-4B: mean attention heads /MLPs in the top- K % circuit.

Task	1%	10%	20%	30%
Addition	0.2/11.8	84.3/34.7	202.6/35.4	321.5/35.5
ARC (Challenge)	0.0/12.0	88.1/30.9	204.6/33.4	322.6/34.4
ARC (Easy)	0.0/12.0	87.6/31.4	204.2/33.8	322.4/34.6
Boolean	0.1/11.9	88.9/30.1	205.8/32.2	323.5/33.5
IOI	0.0/12.0	85.8/33.2	202.7/35.3	321.4/35.6
CopyColors MCQA	0.0/12.0	86.9/32.1	203.8/34.2	322.3/34.7

Table 13. Qwen3-8B: mean attention heads /MLPs in the top- K % circuit.

Task	1%	10%	20%	30%
Addition	0.3/11.7	83.5/35.5	202.2/35.8	321.1/35.9
ARC (Challenge)	0.0/12.0	85.0/34.0	203.1/34.9	321.8/35.2
ARC (Easy)	0.0/12.0	84.7/34.3	203.0/35.0	321.8/35.2
Boolean	0.0/12.0	87.2/31.8	204.4/33.6	322.6/34.4
IOI	0.0/12.0	85.2/33.8	202.6/35.4	321.2/35.8
CopyColors MCQA	0.0/12.0	84.4/34.6	202.9/35.1	321.6/35.4

Checkpoint	Addition	ARC (Challenge)	ARC (Easy)	Boolean	IOI	CopyColors	MCQA
0B	0	0	0	0	0	0	0
3B	0	0	0	0	0	0	0
5B	0	0	0	0	0	0	0
9B	0	0	0	0	0	0	0
17B	50	50	50	0	0		50
32B	50	0	50	0	0		0
53B	50	0	0	0	0		0
76B	0	0	0	0	0		50
399B	0	0	0	0	0		0
797B	0	0	0	0	0		0
1196B	0	0	0	0	0		0
1594B	0	0	0	0	0		0
1993B	0	0	0	0	0		0
2391B	0	0	0	0	0		0
2790B	0	0	0	0	0		0
3209B	0	0	0	0	0		0
3608B	0	0	0	0	0		0
4001B	0	0	0	0	0		0
anneal1 +51B	0	0	0	0	0		0
anneal3 +51B	0	0	0	0	0		0

Table 14. Pretraining **reuse@95 (%)** at $K = 1\%$ across OLMo-2-1B checkpoints. `annealN` entries are stage-2 anneal checkpoints (ingredient N).

Checkpoint	Addition	ARC (Challenge)	ARC (Easy)	Boolean	IOI	CopyColors	MCQA
0B	54	54	46	54	54		54
3B	23	54	54	23	15		54
5B	15	54	54	15	0		46
9B	8	38	31	8	31		31
17B	15	15	15	8	54		15
32B	15	8	8	23	31		15
53B	15	8	8	8	23		46
76B	8	8	8	8	15		38
399B	0	0	0	0	23		8
797B	8	8	8	0	23		8
1196B	8	15	15	0	15		15
1594B	8	15	15	0	15		15
1993B	8	15	23	0	15		23
2391B	8	23	23	0	15		23
2790B	0	23	23	0	23		15
3209B	0	0	0	0	23		0
3608B	0	0	0	0	15		0
4001B	0	0	0	0	0		8
anneal1 +51B	0	23	15	0	0		23
anneal3 +51B	0	15	15	0	0		23

Table 15. Pretraining **reuse@95 (%)** at $K = 5\%$ across OLMo-2-1B checkpoints. `annealN` entries are stage-2 anneal checkpoints (ingredient N).

Checkpoint	Addition	ARC (Challenge)	ARC (Easy)	Boolean	IOI	CopyColors	MCQA
0B	56	56	56	56	56		59
3B	52	56	52	52	48		56
5B	52	52	52	52	48		56
9B	52	56	56	52	56		56
17B	56	56	56	56	63		59
32B	59	56	56	56	59		59
53B	52	56	56	52	56		59
76B	26	56	56	41	48		67
399B	7	15	19	0	33		48
797B	19	33	37	0	22		41
1196B	19	33	33	0	26		41
1594B	15	33	33	0	30		37
1993B	15	33	37	0	33		37
2391B	15	33	33	0	33		41
2790B	15	30	33	0	30		44
3209B	15	37	33	0	26		30
3608B	15	26	30	0	33		48
4001B	7	33	33	0	37		41
anneal1 +51B	15	30	33	0	19		33
anneal3 +51B	22	37	33	0	19		37

Table 16. Pretraining **reuse@95** (%) at $K = 10\%$ across OLMo-2-1B checkpoints. `annealN` entries are stage-2 anneal checkpoints (ingredient N).

Checkpoint	Addition	ARC (Challenge)	ARC (Easy)	Boolean	IOI	CopyColors	MCQA
0B	28	30	30	28	28		30
3B	28	28	28	28	28		31
5B	28	30	28	28	31		33
9B	33	30	30	28	37		33
17B	37	35	33	31	43		37
32B	31	35	35	30	46		35
53B	31	31	30	30	43		37
76B	35	31	33	28	41		39
399B	31	33	35	17	33		44
797B	31	28	26	22	44		37
1196B	31	30	30	20	39		33
1594B	30	28	28	15	41		31
1993B	30	30	28	17	33		35
2391B	28	26	26	17	33		33
2790B	30	30	30	17	30		37
3209B	28	28	28	13	33		33
3608B	30	26	26	9	28		31
4001B	28	28	26	7	30		33
anneal1 +51B	35	26	24	7	28		30
anneal3 +51B	31	28	26	9	28		35

Table 17. Pretraining **reuse@95** (%) at $K = 20\%$ across OLMo-2-1B checkpoints. `annealN` entries are stage-2 anneal checkpoints (ingredient N).

Checkpoint	Addition	ARC (Challenge)	ARC (Easy)	Boolean	IOI	CopyColors	MCQA
0B	19	20	20	19	20		20
3B	20	23	23	19	20		28
5B	22	25	26	19	23		30
9B	27	25	26	22	32		28
17B	31	28	27	30	33		32
32B	30	28	28	26	38		33
53B	28	28	28	26	36		35
76B	28	26	28	21	31		36
399B	42	31	31	19	31		38
797B	31	21	21	19	33		32
1196B	27	23	25	17	36		37
1594B	27	21	22	14	36		31
1993B	30	27	27	15	35		28
2391B	27	22	23	16	32		31
2790B	30	25	25	15	33		32
3209B	30	26	26	15	35		30
3608B	30	23	25	11	33		30
4001B	30	23	25	11	33		30
anneal1 +51B	32	22	22	9	37		30
anneal3 +51B	31	23	23	11	36		36

Table 18. Pretraining reuse@95 (%) at $K = 30\%$ across OLMo-2-1B checkpoints. annealN entries are stage-2 anneal checkpoints (ingredient N).

Checkpoint	Addition	ARC (Challenge)	ARC (Easy)	Boolean	IOI	CopyColors	MCQA
0B	-	0.00	0.00	0.00	0.00	0.00	
3B	0.00	0.00	0.00	0.00	0.00	0.00	
5B	-	0.00	0.00	0.00	0.00	0.00	
9B	-	0.00	0.00	0.00	0.00	0.00	
17B	-	-0.10	0.00	0.00	0.00	0.00	
32B	-	0.00	-0.40	0.00	0.00	0.00	
53B	-	0.00	0.00	0.00	0.00	0.00	
76B	-	0.00	0.00	0.00	0.00	-2.00	
399B	0.00	0.00	0.00	0.00	0.00	0.00	
797B	-	0.00	0.00	0.00	0.00	0.00	
1196B	0.00	0.00	0.00	0.00	0.00	0.00	
1594B	0.00	0.00	0.00	0.00	0.00	-	
1993B	0.00	0.00	0.00	0.00	0.00	0.00	
2391B	0.00	0.00	0.00	0.00	0.00	0.00	
2790B	0.00	0.00	0.00	0.00	0.00	0.00	
3209B	0.00	0.00	0.00	0.00	0.00	-	
3608B	0.00	0.00	0.00	0.00	0.00	0.00	
4001B	0.00	0.00	0.00	0.00	0.00	0.00	
anneal1 +51B	0.00	0.00	0.00	0.00	0.00	0.00	
anneal3 +51B	0.00	0.00	0.00	0.00	0.00	0.00	

Table 19. Pretraining necessity at $K = 1\%$ across OLMo-2-1B checkpoints. annealN entries are stage-2 anneal checkpoints (ingredient N).

Checkpoint	Addition	ARC (Challenge)	ARC (Easy)	Boolean	IOI	CopyColors	MCQA
0B	–	0.21	-0.06	-0.04	-0.10	-0.50	
3B	0.00	0.07	0.22	-0.03	-0.06	0.00	
5B	–	0.06	-0.04	-0.04	0.00	0.00	
9B	–	0.00	-0.04	0.26	0.03	0.00	
17B	–	0.03	0.00	-0.10	-0.55	0.00	
32B	–	-0.65	-0.19	0.02	-0.75	0.00	
53B	–	-0.18	0.00	0.01	-0.63	0.00	
76B	–	-0.38	-0.07	0.00	-0.10	-1.00	
399B	0.00	0.00	0.00	0.00	-0.19	-0.75	
797B	–	0.48	-0.10	0.00	-0.18	0.00	
1196B	0.00	0.27	0.16	0.00	0.06	-0.50	
1594B	0.00	0.03	0.10	0.00	-0.16	–	
1993B	0.00	0.05	-0.15	0.00	-0.03	-1.00	
2391B	0.00	-0.06	-0.05	0.00	-0.22	-3.00	
2790B	0.00	-0.33	-0.02	0.00	0.05	0.00	
3209B	0.00	0.00	0.00	0.00	0.19	–	
3608B	0.00	0.00	0.00	0.00	-0.25	0.00	
4001B	0.00	0.00	0.00	0.00	0.00	1.00	
anneal1 +51B	0.00	-0.11	0.28	0.00	0.00	0.78	
anneal3 +51B	0.00	0.42	0.32	0.00	0.00	0.50	

Table 20. Pretraining necessity at $K = 5\%$ across OLMo-2-1B checkpoints. `annealN` entries are stage-2 anneal checkpoints (ingredient N).

Checkpoint	Addition	ARC (Challenge)	ARC (Easy)	Boolean	IOI	CopyColors	MCQA
0B	–	-0.18	-0.23	0.04	0.04	0.00	
3B	0.00	-0.03	-0.24	-0.02	-0.02	0.00	
5B	–	0.33	0.04	-0.06	-0.03	-0.50	
9B	–	-0.08	-0.12	-0.04	-0.30	1.00	
17B	–	-0.10	-0.16	0.35	-0.04	0.00	
32B	–	-0.26	-0.40	0.02	-0.72	-0.33	
53B	–	-0.27	-0.37	0.23	-0.31	0.25	
76B	–	-0.42	-0.30	0.09	-1.17	-2.00	
399B	0.00	-0.17	0.24	0.00	-0.58	0.75	
797B	–	-0.08	0.10	0.00	-0.29	0.00	
1196B	0.00	0.00	0.12	0.00	-0.04	0.00	
1594B	0.00	0.03	0.00	0.00	-0.33	–	
1993B	0.00	0.00	0.06	0.00	-0.58	0.00	
2391B	0.00	0.15	-0.12	0.00	-0.04	1.00	
2790B	0.00	-0.14	0.16	0.00	-0.73	0.00	
3209B	0.00	-0.17	0.07	0.00	0.12	–	
3608B	0.00	-0.28	0.04	0.00	0.01	-1.33	
4001B	0.00	-0.03	0.11	0.00	-0.18	2.00	
anneal1 +51B	0.00	0.00	-0.03	0.00	-0.27	0.33	
anneal3 +51B	0.00	-0.06	-0.05	0.00	-0.62	0.30	

Table 21. Pretraining necessity at $K = 10\%$ across OLMo-2-1B checkpoints. `annealN` entries are stage-2 anneal checkpoints (ingredient N).

Checkpoint	Addition	ARC (Challenge)	ARC (Easy)	Boolean	IOI	CopyColors	MCQA
0B	–	0.00	-0.23	0.04	0.04	0.00	
3B	0.00	-0.03	-0.08	-0.07	-0.06	-0.50	
5B	–	0.19	-0.12	-0.58	-0.27	-0.50	
9B	–	-0.08	-0.12	0.00	0.02	1.00	
17B	–	0.03	0.07	0.31	-0.05	-0.50	
32B	–	0.00	0.05	0.02	-0.16	-0.33	
53B	–	-0.32	-0.42	0.43	-0.24	0.25	
76B	–	-0.42	-0.30	0.43	-0.41	-2.00	
399B	0.00	-0.35	-0.16	-0.14	-0.26	1.00	
797B	–	-0.04	-0.33	0.42	0.10	0.00	
1196B	0.00	0.09	-0.36	0.02	-0.56	0.50	
1594B	0.00	-0.06	0.02	-0.03	0.04	–	
1993B	0.00	0.00	0.29	0.48	-0.51	-0.50	
2391B	0.00	-0.26	0.21	0.01	-0.58	-3.00	
2790B	0.00	-0.17	-0.20	0.00	0.04	1.00	
3209B	0.00	0.08	0.07	0.21	0.00	–	
3608B	0.00	-0.04	0.08	0.03	-0.08	-0.67	
4001B	0.00	-0.15	-0.09	-0.06	-0.04	1.00	
anneal1 +51B	0.00	0.06	0.15	0.01	-0.02	0.78	
anneal3 +51B	0.00	-0.13	0.03	-0.21	0.04	0.70	

Table 22. Pretraining necessity at $K = 20\%$ across OLMo-2-1B checkpoints. `annealN` entries are stage-2 anneal checkpoints (ingredient N).

Checkpoint	Addition	ARC (Challenge)	ARC (Easy)	Boolean	IOI	CopyColors	MCQA
0B	–	0.00	-0.23	0.04	0.02	0.00	
3B	1.00	-0.03	-0.08	-0.07	-0.06	-0.50	
5B	–	0.19	-0.12	-0.58	-0.27	-0.50	
9B	–	-0.08	-0.12	0.00	0.02	1.00	
17B	–	0.03	0.07	0.31	-0.05	-0.50	
32B	–	0.00	0.05	0.01	-0.16	-0.33	
53B	–	-0.32	-0.42	0.43	-0.24	0.25	
76B	–	-0.42	-0.30	0.43	-0.41	-2.00	
399B	0.00	-0.74	-0.11	0.36	0.37	1.00	
797B	–	0.32	-0.05	0.51	0.10	0.00	
1196B	0.33	-0.36	-0.30	0.32	0.01	0.50	
1594B	1.00	0.00	-0.08	-0.03	0.04	–	
1993B	0.00	0.03	0.02	0.45	-0.11	-0.50	
2391B	0.00	-0.06	-0.14	0.30	-0.28	-3.00	
2790B	0.00	-0.11	-0.10	0.36	-0.21	1.00	
3209B	0.00	0.00	0.02	0.04	-0.15	–	
3608B	0.00	-0.16	0.02	0.09	-0.06	0.00	
4001B	0.00	-0.03	0.18	0.00	-0.03	1.00	
anneal1 +51B	0.00	0.40	0.68	0.11	-0.22	0.78	
anneal3 +51B	0.00	0.21	0.57	0.28	-0.05	0.70	

Table 23. Pretraining necessity at $K = 30\%$ across OLMo-2-1B checkpoints. `annealN` entries are stage-2 anneal checkpoints (ingredient N).